

GPS REPORTS

Effects of Transmission Lines on Global Positioning Systems

Prepared by:

Pollock & Wright

&

Manitoba Hydro DC-Line GNSS Survey Report

Prepared by:

PLAN Group

Effects of Transmission Lines On Global Positioning Systems



LAND SURVEYING • GEOMATICS

117 FORT STREET, WINNIPEG, MB R3C 1C6

TABLE OF CONTENTS

1.0	Scope of Work	1
2.0	Equipment Used.....	1
3.0	Network Design/ Test Location	1
4.0	Observations.....	3
5.0	Results	7
6.0	Conclusions.....	10
7.0	Definitions.....	11

1.0 Scope of Work

The intent of the project was to determine if Global Positioning Systems (GPS) signals or any associated radio correction signal corrections to GPS signals (Differential GPS operation) experienced any interference in close proximity to high voltage power lines. The test involved taking measurements with three GPS receivers under Direct Current (DC) and Alternating Current (AC) transmission lines.

2.0 Equipment Used

Five GPS receivers were used along with three different radio correction methods. Two 4000 SSE Trimble Dual Frequency receivers, one 5700 Trimble Dual Frequency Receiver and two R8 GNSS Trimble Dual Frequency Receivers were used for this test. An internal Trimtalk radio broadcasting on 440.4 MHZ was used to supply differential GPS corrections. Differential corrections were also received from a wide area network hookup via a cellphone/internet link as well as Wide Area Augmentation System (WAAS) corrections.

3.0 Network Design/Test Location

The test location was along PR# 322 located North of Grosse Isle, Manitoba. At the location there were two High Voltage DC transmission lines (Bipoles I and II) and an AC line. Two points were placed well away from the transmission line (Points 1 and 3), while three others were located directly under the middle transmission line, with two of these points being placed in close proximity to existing towers (Points 2 and 4), and the other being placed directly under the lowest point of the transmission line (Point 5). A sixth point was placed close to a tower and directly under an AC line, (Point 6). In order to assess the integrity of the network the location of all points were confirmed with a Wild 805 Total Station using conventional survey methods. The conventional survey measurements established points to within 5mm and form a reference base that was unaffected by any outside influences. Figure 1 shows the test environment and Figure 2 the network configuration. All observations were carried out between 8AM and 6PM when the lines were energized.

Effects of Transmission Lines on GPS



Figure 1
Test Environment



Figure 2
Network Configuration

4.0 Observations

4.1 Reference Framework – In order to establish a framework that would allow for the evaluation of the effects of the transmission lines on GPS and any GPS correction signals which were being transmitted by Radio Frequencies (RF), a reference framework that was not subject to any RF interference was created. A series of points were established at locations directly under and adjacent to the existing transmission lines, as well as some points were placed away from the transmission lines. Three of the points were also placed in close proximity to existing towers to see if the towers themselves would cause any problems either through multipath of the GPS signals or actual signal blockage. Figure 2 identifies the location of points established. The points were all measured with a LEICA 805 Total Station using conventional angle and distance measurements between the stations. Using these measurements coordinates were established for each point.

4.2 GPS Observations – Several forms of GPS observations were carried out.

4.3 Static Observations - Static GPS observations are observations where GPS receivers are placed at each point for an extended period of time. The carrier phase of the GPS signals were sampled at 10 second intervals over a one hour period. The data was then subsequently post processed via TRIMBLE's™ Geomatic Office Wave Baseline processing engine. Both frequencies of the GPS carrier phase L1 (1575.42 MHz) and L2 (1227.6 Mhz) were sampled during this observation period. All baselines that were processed passed the baseline screening tests imposed by the software, which is meant to detect and reject data that is outside of what is expected. Only points 1 to 5 were observed using static techniques. Point 6 was placed under the AC line which was not originally to be included in the scope of the project.

Nine baselines were generated from the processing with all of them generating acceptable solutions. A baseline processing summary can be seen in Table 1.

Satellite tracking for all of the observations on all of the satellites indicated no interference was present at the time of the observations.

Table 1
GPS Static Baseline Summary

Processing Summary

ID	From	To	Baseline Length	Solution Type	Ratio	Reference Variance	RMS
B4	3	2	305.432m	L1 fixed	40.1	2.478	0.005m
B1	3	4	315.208m	L1 fixed	19.4	2.686	0.007m
B5	3	1	443.533m	L1 fixed	40.7	1.382	0.005m
B2	2	4	302.823m	L1 fixed	4.0	3.551	0.008m
B6	2	1	328.608m	L1 fixed	33.5	2.238	0.006m
B3	4	1	145.724m	L1 fixed	3.0	2.933	0.007m
B92	3	5	271.694m	L1 fixed	24.6	0.997	0.004m
B93	3	1	443.547m	L1 fixed	13.0	0.976	0.004m

A sample of a typical satellite tracking session is provided in Figure 3. It can be observed that the observations had a mean value of 0.001m (1 mm) with a minimum and maximum value of 0.013 M (13 mm) over the length of the observation. This was seen to be typical of all observations regardless if they were located under or away from the transmission lines.

Effects of Transmission Lines on GPS

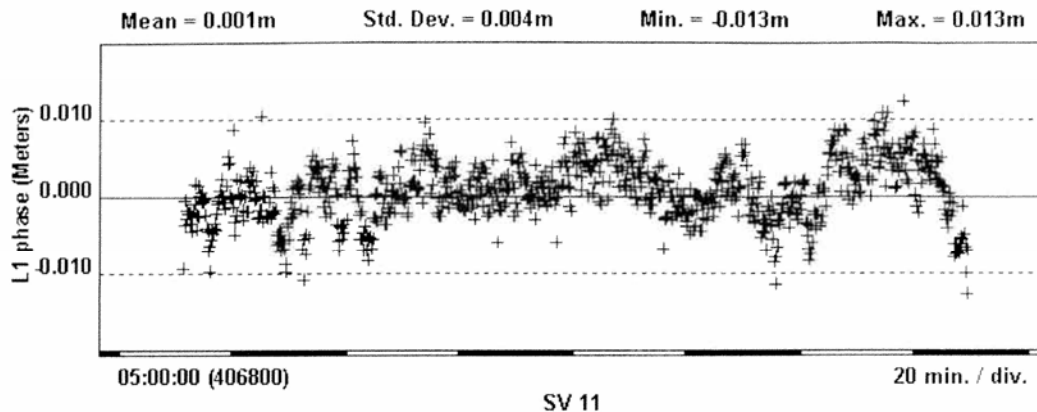


Figure 3
Typical Satellite Carrier Phase Tracking

Real Time Kinematic Observations (RTK) - These are GPS observations that are carried out as the name implies in Real Time and can yield positions of points relative to one another in the centimeter range. To establish a Real Time GPS survey one receiver has to be placed on a point and it has to remain at this point for the duration of the survey. This receiver is designated as the base. The base station re-broadcasts the phase of the GPS carrier wave that it has measured over a radio link. This is usually done using a UHF radio modem. For our test the UHF radio had a frequency of 440.4 MHz. Mobile GPS units, typically called rovers, compare their own phase measurements with the ones received from the base and a correction is generated in the rover that allows its position to be corrected to within a few centimeters relative to the base station receiver. This application is very common in survey grade RTK equipment, as well as some high end precision farming equipment.

In order to assess the influence of the transmission lines a base receiver was set up at point 3, well away from the hydro line. A rover receiver was then taken to each point in the network and a coordinate for the point was observed and recorded. All of the observations were carried out using the Trimble™ R8 GNSS receiver. The observations were repeated several times using a variety of satellite configurations and observations. The R8 receiver is capable of tracking all of the GPS carrier phases plus the Russian Glonass satellite system. Coordinates for the points were observed with the following: L1 Carrier Phase GPS only, L1 and L2 Carrier Phase GPS only, L1 and L2 GPS plus Glonass Carrier phase.

An observation session was repeated with the base station set up on point 4 which was directly under the transmission lines and in close proximity to a steel lattice tower.

Real Time Kinematic Observations using a wide area network – All of the points were observed using a TRIMBLE™ 5700 GPS receiver connected to a wide area reference network via a cell phone and internet link. The wide area network consists of many

Effects of Transmission Lines on GPS

permanent GPS stations that are located throughout Southern Manitoba. These stations are sampling the GPS signals on a 1 second interval and all of the data is fed back to a central server which supplies Real Time Kinematic Corrections to rovers the same way as if a base station was established at the project site. The only difference is that the corrections are being supplied over a cell phone link and internet connection.

Real Time Kinematic using WAAS - Observations were carried out on the points established utilizing the WAAS System. Typically the corrections supplied in a WAAS application yield positions to accurate to within 0.5 to 1 metre. A typical GPS RTK rover observation is given in Figure5 below.



Figure 4
Typical RTK Observation

5.0 Results

The coordinates for the reference points were generated by all of the methods used to observe the network. Table 2 shows the values obtained; in addition to carrying out observations on the established network points it was observed that at no time in the surveys did the GPS receivers experience loss of satellite lock or system integrity (loss of initialization) despite working directly under the transmission lines and adjacent to the towers. It should be noted that a fast static observation was not carried out on point 6 as this was under the AC line and the initial test was to be performed around the DC lines which are similar to the proposed Bipole III line.

**Table #2
Conventional Values- Reference Coordinates**

Point #	Northing	Easting	Elevation	Description
1	10000.000	10000.000	221.665	PL 0.013 RD IP
2	10319.517	9923.242	220.821	PL 0.013 RD IP
3	10384.110	10221.766	220.425	PL 0.013 SQ IP
4	10086.818	10117.020	219.545	PL 0.013 RD IP
5	10197.948	10023.888	221.055	PL 0.013 RD IP
6	10279.694	9873.818	219.855	PL 0.013 RD IP

Table 3 provides the values obtained for the stations using Fast Static GPS only techniques. The differences in the table are in metres and show the comparison to the conventional measurements.

**Table #3
Static GPS Observations –L1 and L2 Carrier Phase Data**

Point #	Northing	Easting	Elevation	Delta X	Delta Y	Delta Z
1	10000.007	10000.002	221.672	-0.007	-0.002	-0.007
2	10319.514	9923.246	220.825	0.003	-0.004	-0.004
3	10384.104	10221.760	220.425	0.004	0.006	0.0000
4	10086.820	10117.019	219.542	-0.002	0.001	0.003
5	10197.953	10023.891	221.056	-0.005	-0.003	-0.001
6	Not Observed	Not Observed				

Effects of Transmission Lines on GPS

Table 4 gives the values obtained using Real Time Kinematic Techniques with observations on both GPS and Glonass Satellites and the base station set up on Point #3 which is well away from the hydro lines.

Table #4 GPS and Glonass

Point#	Northing	Easting	Elevation	Delta X	DeltaY	Delta Z
1	9999.994	10000.008	221.671	0.006	-0.008	-0.006
2	10319.526	9923.238	220.828	-0.009	0.003	-0.007
3	10384.112	10221.768	220.424	-0.002	-0.002	0.001
4	10086.818	10117.010	219.543	0.000	0.011	0.002
5	10197.943	10023.892	221.057	0.005	-0.004	-0.002
6	10279.690	9873.811	219.856	0.004	0.007	-0.001

Table 5 gives the values obtained using Real Time Kinematic Techniques with observations on GPS satellites only. The Base station was established at point #3.

Table #5 GPS Only

Point #	Northing	Easting	Elevation	Delta X	Delta Y	Delta Z
1	10000.004	10000.001	221.672	-0.004	-0.001	-0.007
2	10319.523	9923.240	220.820	-0.006	0.002	0.001
3	10384.113	10221.760	220.423	-0.003	0.006	0.002
4	10086.804	10117.018	219.543	0.013	0.002	0.002
5	10197.949	10023.898	221.051	-0.001	-0.010	0.004
6	Not Observed	Not Observed				

Table 6 gives the values obtained using Real Time Kinematic Techniques with observations on the GPS satellites using only the L1 frequency (single frequency). The base station at Point #3.

Table #6 GPS (L1 Only)

Point #	Northing	Easting	Elevation	Delta X	Delta Y	Delta Z
1	10000.00433	9999.995377	221.666	-0.004	0.005	-0.001
2	10319.52517	9923.241756	220.822	-0.008	0.000	-0.001
3	10384.1127	10221.75999	220.423	-0.003	0.006	0.002
4	10086.8112	10117.02758	219.548	0.006	-0.007	-0.003
5	10197.93914	10023.89124	221.051	0.009	-0.003	0.004

Effects of Transmission Lines on GPS

Table 7 gives the values obtained using WAAS corrections. Note Base point # 3 was not observed for this scenario as it had the local base occupied on it at the time of observation.

Table #7 WAAS

Point #	Northing	Easting	Elevation	Delta X	Delta Y	Delta Z
1	10000.011	10000.500	222.670	-0.011	-0.500	-1.05
2	10319.716	9923.738	222.321	-0.199	-0.496	-1.500
3	Not Observed	Not Observed				
4	10086.409	10117.723	219.839	0.409	-0.003	-0.703
5	10197.656	10024.890	222.057	0.292	-1.002	-1.002

Table 8 gives values obtained using GPS and Glonass satellites in Real Time Kinematic mode with the base station set up on Point #4, which is directly under the hydro lines and in close proximity to a hydro tower.

Table #8 Base at Point 4

Point #	Northing	Easting	Elevation	Delta X	Delta Y	Delta Z
1	10000.009	9999.998	221.667	-0.009	0.002	-0.002
2	10319.527	9923.244	220.815	-0.011	-0.002	0.006
3	10384.115	10221.761	220.436	-0.005	0.005	-0.009
4	10086.807	10117.018	219.545	0.011	0.002	0.000
5	10197.944	10023.890	221.059	0.004	-0.002	-0.004
6	10279.684	9873.823	219.850	0.010	-0.005	0.005

Table 9 gives values obtained using GPS only with corrections supplied from a remote base and the corrections are applied via a cell phone and internet connection. Point #6 was not observed.

Table #9 Network Solution/Cellphone Corrections

Point #	Northing	Easting	Elevation	Delta X	Delta Y	Delta Z
1	10000.006	10000.003	221.659	-0.006	-0.003	0.006
2	10319.524	9923.234	220.831	-0.007	0.008	-0.010
3	10384.107	10221.766	220.427	0.003	0.000	-0.002
4	10086.808	10117.025	219.534	0.009	-0.005	0.011
5	10197.948	10023.889	221.032	0.000	-0.001	0.023

6.0 Conclusions

The differences between the ground truth positions established using conventional survey methods and the GPS observations indicate that transmission lines that supply Direct Current have no appreciable effect on either GPS measurements or ultra high frequency radios/cell phones that supply GPS correction messages. The results obtained were well within the manufacturers quoted equipment accuracies (i.e., centimeter level).

It should be noted that over the course of the day we experienced no loss of initialization in the GPS equipment, nor did we have any trouble initializing the equipment after we intentionally dropped satellite lock or when we started another observation session. If the transmission lines were to have an effect it typically would be noticed when re-initialization was to occur, as any interference would make solving the integer ambiguity for the GPS carrier phase very difficult, whether it was due to satellite lock failure or communication loss.

We also noticed that radio and cell phone links performed consistently over the course of the day. The RTK equipment will put out messages when communication is lost from whatever base station is being used to supply the real time correction messages to notify the user that loss of communication has occurred. We had no messages that the communication link was ever lost.

We also noticed that the adjacent AC transmission line did not cause any problems during this observation period. We established point 6 under this line and had similar results as those under the Direct Current Line. We carried out additional kinematic observations under the AC line and experienced no problems.

7.0 Definitions

Ambiguity (or integer bias term) - The unknown number of whole wavelengths of the carrier signal contained in an unbroken set of measurements between a receiver and a GNSS satellite. This number can be solved for by making successive measurements of the carrier phase of GPS transmissions. Essentially for centimeter level positioning.

Carrier Frequency (Phase) – Frequency of the unmodulated output of a radio transmitter/GNSS satellite. L1-1575.42 MHZ (19 cm. Wavelength) and L2- 1227.60 MHZ (24 cm. wavelength)

GPS - Global Positioning System consisting of 32 satellites that transmit radio messages imposed on a carrier frequency. Maintained by the United States of America.

Glonass - Global Positioning System consisting of 26 satellites that transmit radio messages imposed on a carrier frequency. Maintained by the USSR.

GNSS - Global Navigation Satellite System

Real Time Kinematic - A position location process whereby signals received from a reference device (such as a GPS receiver) can be compared using carrier phase corrections from a reference station to the user's roving receiver.

Static GPS – Carrier phase differencing technique where the integer ambiguities (numbers) are resolved from extended observation periods through a change in satellite Geometry. It is the highest accurate form of GPS measurement.

WAAS - Wide Area Augmentation System - A system of earth stations and satellites that improves the tracking accuracy of the GPS navigation system to approximately 10 feet. Deployed in 2003, WAAS comprises a group of 25 reference stations and two satellites that cover North America. The stations track the GPS satellites and send correction signals to the WAAS satellites, which transmit them to WAAS-enabled receivers.



MANITOBA HYDRO DC-LINE GNSS SURVEY REPORT

Prepared for

Manitoba Hydro
Attn: A.E. Pinder - Manager
Communications Department
820 Taylor Avenue
Winnipeg, Manitoba R3M 3T1
Tel: 204-360-3868, apinder@hydro.mb.ca

by

PLAN Group
Department of Geomatics Engineering
The University of Calgary
2500 University Drive NW
Calgary, T2N 1N4

Professor Gérard Lachapelle
Tel: 403 220 7104, Gerard.Lachapelle@ucalgary.ca

Senior Research Engineers:
Dr. Jared Bancroft - Tel: 403 210 9802, j.bancroft@ucalgary.ca
Dr Aiden Morrison - Tel: 403 210 9797, ajmorrison@ucalgary.ca

March 11, 2011
(Revised: June 4, 2011)

Executive Summary

Manitoba Hydro requires an independent study to analyze the ability of Global Navigation Satellite System (GNSS) receivers to operate under high voltage direct current power lines. On Jan 24th and Jan 25th, 2011, data was collected by the PLAN Group of the University of Calgary under two High Voltage DC power lines located in Manitoba. Two survey grade GNSS receivers collected data, one of which functioned with a real time data link; survey grade receivers are typically the ones used for precision farming; they use both delay lock loops and phase lock loops to make pseudorange and carrier phase measurements, respectively. Phase lock loop measurements are very accurate but are more sensitive to interference. Raw intermediate frequency data was also collected and processed using GSNRx™ to examine the characteristics of pseudorange and carrier phase measurements at the fundamental level; GSNRx™ is a software receiver capable of monitoring the behavior of the incoming satellite signals (Petovello et al 2009); a High Sensitivity GPS receiver also collected data; this type of receiver uses delay lock loop measurements.

This report concludes that very minor adverse effects on GNSS receiver performance and incoming signals could be measured or detected from either the overhead lines or the towers that support the actual lines. The latter effect is due to reflection or brief masking by the towers. This conclusion is based on an analysis of the position accuracy, HDOP, number of satellites tracked, code and phase residual errors, location and number of cycle slips, carrier-to-noise density and L1-L2 carrier divergence. Four different processing software packages were used to process the data collected by the receivers and all provided consistent results confirming that the GNSS data as collected by the receivers had not been compromised.

Table of Contents

Executive Summary	ii
Table of Contents	iii
List of Figures	v
List of Tables	ix
1 Project Description.....	1
1.1 Purpose	1
1.2 Methodology and Equipment Used	1
1.2.1 Commercially Available GNSS Receivers.....	1
1.2.2 GNSS Baseband Data	2
1.3 Project Timeline.....	2
2 Field Setup and Testing.....	4
2.1 Base Station Deployment.....	4
2.2 Rover GNSS and HSGPS Deployment.....	5
2.3 Reference INS Deployment.....	7
2.4 Rover RF Front-End Deployment.....	7
3 Data Evaluation	11
3.1 Reference Solution Evaluation	12
3.2 Differential GNSS Observations	14
3.2.1 Trimble RTK Analysis.....	14
3.2.2 NovAtel Receiver Analysis	19
3.2.2.1 Received Signal Power	19
3.2.2.2 Position Errors and Satellite Geometry	21
3.2.2.3 Residual Errors.....	23
3.2.3 Carrier Phase Cycle Slip Analysis.....	25
3.3 RF Front-End Measurement Analysis	29
3.4 HSGPS Observations.....	36

4	Conclusions	39
5	References	40

List of Figures

Figure 1 – Project timeline	3
Figure 2 – Deployment of GNSS base stations on 24 January 2011. Novatel V3 receiver utilizes right tripod equipped with a Novatel 702-GG GPS+GLONASS L1+L2 antenna. Trimble R8 base unit occupies left tripod, with integrated receiver + antenna + radio module. Radio antenna is the black vertical bipole antenna visible under the R8 receiver body.	4
Figure 3 – Map of test location showing location of the V3 base stations for each day (green triangles), range of Trimble R8 450 MHz data link (blue circle), and position of DC bipole 1 and 2 (black lines), position of AC Line (green lines). Base map from Google (2011).	5
Figure 4 – Mobile GNSS, Inertial, and RF equipment elements mounted on roof of test vehicle. Trimble R8 rover unit at bottom right, high sensitivity GPS antennas on roof at right, Novatel 702 GG dome antenna centre left directly adjacent to LCI IMU (grey box) at centre left.	6
Figure 5 – Deployed equipment functional diagram. Equipment external to vehicle shown as olive green elements (antennas, IMU, Trimble R8), equipment installed inside vehicle shown in blue. Cabled RF links shown with blue arrows, digital data links shown with green arrows.	6
Figure 6 – Estimated Standard Deviation (1σ) of the Reference Trajectory as Output by Inertial Explorer.....	13
Figure 7 – Difference in IMU Mechanization Positions and GNSS Positions as Output by Inertial Explorer.....	14
Figure 8 – Position Errors and Satellite Geometry, Receiver: Trimble R8, Processed by: Trimble Internal RTK Solution, Data: L1+L2+GPS+GLONASS, Test Segment: 14	15
Figure 9 – Position Error and Satellite Geometry, Receiver: Trimble R8, Processed by: Trimble Internal RTK Solution, Data: L1+L2+GPS+GLONASS, Test Segment: 19	17

Figure 10 – Position Errors and Satellite Geometry, Receiver: Trimble R8, Processed by: NovAtel’s GrafNav, Data: L1+L2+GPS, Test Segment: 14 18

Figure 11 – Position Error and Satellite Geometry, Receiver: Trimble R8, Processed by: NovAtel’s GrafNav, Data: L1+L2+GPS, Test Segment: 19 19

Figure 12 – GNSS Signal Strength, Receiver: NovAtel V3, Data: L1+L2+GPS+GLONASS, Test Segment: 14 20

Figure 13 – GNSS Signal Strength, Receiver: NovAtel V3, Data: L1+L2+GPS+GLONASS, Test Segment: 19 21

Figure 14 – Position Error and Satellite Geometry, Receiver: NovAtel V3, Processed by: PLANSoft, Data: L1+GPS+GLONASS, Test Segment: 14 22

Figure 15 – Position Error and Satellite Geometry, Receiver: NovAtel V3, Processed by: PLANSoft, Data: L1+GPS+GLONASS, Test Segment: 19 22

Figure 16 – RMS of Residuals, Receiver: NovAtel V3, Processed by: PLANSoft, Data: L1+GPS+GLONASS, Test Segment: 14 24

Figure 17 – RMS of Residuals, Receiver: NovAtel V3, Processed by: PLANSoft, Data: L1+GPS+GLONASS, Test Segment: 19 24

Figure 18 – Geo-Located Cycle Slips (red: 24 Jan, purple: 25 Jan), blue rectangles indicate Figure 19, Figure 20 and Figure 21 26

Figure 19 – Geo-Located Cycle Slips (red: 24 Jan, purple: 25 Jan) 27

Figure 20 – Geo-Located Cycle Slips (red: 24 Jan, purple: 25 Jan) 28

Figure 21 – Geo-Located Cycle Slips (red: 24 Jan, purple: 25 Jan) 28

Figure 22 – Test segment 1 perpendicular crossing of power line corridor effect of two DC bipoles and 1 AC transmission line set on L1-L2 phase difference and carrier-to-noise density ratios of GLONASS M satellite in orbital slot 1. Lower L2 signal strength is due to lower transmitted signal strength from satellite in this band relative to L1 and lower gain of 702 GG antenna element at L2 frequencies. Traversal of eastern bipole centreline occurred at approximately 152962 seconds. Trend in carrier divergence is due to slowly changing ionospheric background conditions during test and is expected. 30

Figure 23 – Test segment 1 perpendicular crossing of power line corridor effect of two DC bipoles and 1 AC transmission line set on L1-L2 phase difference and

carrier-to-noise density ratios of GLONASS M satellite in orbital slot 2. Lower L2 signal strength is due to lower transmitted signal strength from satellite in this band relative to L1 and lower gain of 702 GG antenna element at L2 frequencies. Traversal of eastern bipole centreline occurred at approximately 152962 seconds. Trend in carrier divergence is due to slowly changing ionospheric background conditions during test and is expected. 30

Figure 24 – Test segment 1 perpendicular crossing of power line corridor effect of two DC bipoles and 1 AC transmission line set on L1-L2 phase difference and carrier-to-noise density ratios of GPS IIR-M satellite transmitting PRN code 29. Lower L2 signal strength is due to lower transmitted signal strength from satellite in this band relative to L1 and lower gain of 702 GG antenna element at L2 frequencies. Traversal of eastern bipole centreline occurred at approximately 152962 seconds. Trend in carrier divergence is due to slowly changing ionospheric background conditions during test and is expected..... 31

Figure 25 – Test Segment 8, parallel travel along transmission line corridor indicating brief blockage due to transmission towers on GLONASS SV 18. Deep fade on L1 results in multiple cycle slips causing off scale L1-L2 carrier difference, which is an expected result during signal blockage..... 33

Figure 26 – Test Segment 8, parallel travel along transmission line corridor indicating brief blockage due to transmission towers on GLONASS SV 2. Shallow fade on L1 results in no cycle slip. 33

Figure 27 – Test Segment 8, parallel travel along transmission line corridor indicating brief blockage due to transmission towers on GPS PRN 15. No cycle slip occurrence..... 34

Figure 28 – Test Segment 9, parallel travel along transmission line corridor indicating two brief blockages due to transmission towers on GLONASS SV 2. No cycle slip occurrence..... 34

Figure 29 – Test Segment 9, parallel travel along transmission line corridor indicating brief blockage of L2 signal path on GLONASS SV 18. Apparent decrease in carrier strength in both L1 and L2 signals during final static portion

of test believed to be due to change in inclination of GNSS antenna. No cycle slip occurrence..... 35

Figure 30 – Test Segment 9, parallel travel along transmission line corridor indicating brief blockage of L2 signal path on GPS PRN 158. Apparent increase in carrier strength in both L1 and L2 signals during final static portion of test believed to be due to change in inclination of GNSS antenna, increasing directional gain towards SV. No cycle slip occurrence. 35

Figure 31 – Position Error and Satellite Geometry, Receiver: U-blox Antaris 4, Processed by: U-blox Internal Solution, Data: L1+HSGPS, Test Segment: 14 37

Figure 32 – Position Error and Satellite Geometry, Receiver: U-blox Antaris 4, Processed by: U-blox Internal Solution, Data: L1+HSGPS, Test Segment: 19 37

List of Tables

Table 1 – Data Segment Information.....	11
Table 2 – Software Processing Strategies.....	12

1 Project Description

1.1 Purpose

Manitoba Hydro desires an independent study to analyze the ability of Global Navigation Satellite System (GNSS) receivers to operate under high voltage DC (direct current) power lines. Receivers chosen were able to collect data from the Global Positioning System (GPS) and the Russian GLONASS (Global Navigation Satellite System). Potential effects that were considered were the EM field generated by the power lines and signal attenuation from the supporting towers.

The PLAN Group of the University of Calgary conducted data collections in the Winnipeg area on January 24-25, 2011, under DC power lines selected by Manitoba Hydro. Data was analyzed to assess the impact of potential interference on GNSS receivers and centimetre level positioning capabilities. The PLAN Group analyzed the effects using several approaches as discussed in Section 1.2.

1.2 Methodology and Equipment Used

Two receiver configurations were used to collect data, namely (i) commercially available GNSS receivers and (ii) a front-end to collect GNSS baseband data.

1.2.1 Commercially Available GNSS Receivers

Two GNSS base stations, one utilizing a Novatel V3 receiver, the other utilizing a Trimble R8 survey receiver were placed approximately 350 to 500 m from the DC bipoles, where they logged data continuously. The base stations served as reference stations for processing the data in differential mode, a mode commonly used for precise positioning applications such as those encountered in farming and construction. Mobile GNSS equipment was mounted on a vehicle provided by Manitoba Hydro to collect data in roving mode as follows: (1) the vehicle moved at low speeds to simulate that of typical agricultural machinery, namely 10 - 20 km/h, (2) a first trajectory approximately perpendicular to the power lines was traversed on rural route 321 from and to a point approximately 500 m each side of the first DC bipole and (3) a second trajectory running

along the right of way, under and approximately parallel to the transmission lines was taken spanning the distance between three supporting towers.

A total of 19 collection trajectories were executed, including 12 perpendicular tests, 2 static tests directly under the trough of the DC bipole and 5 parallel collection tests.

The mobile equipment installed in the vehicle included five GNSS receiver systems, including a second Novatel V3, a Trimble R8 rover, a high sensitivity u-blox receiver, and a NovAtel SPAN Inertial Navigation System (INS) system, which consisted of an LCI inertial measurement unit (IMU) and a NovAtel SPAN SE GNSS receiver. Since INS are self-contained and are not affected by external signals, they are used to further verify the accuracy and integrity of the GNSS-derived solutions.

The Trimble R8 receiver included an optional data link that received corrections from the nearby R8 base station, as long as the test vehicle remained within approximately 1 km of the base station. Since this data link operates on a frequency separate from the GNSS carrier frequencies, it was tested to ensure continuous operation during a subset of the test runs. The radio link was used on the second day, Tuesday Jan 25th, 2011.

1.2.2 GNSS Baseband Data

The mobile equipment also included a computer-based system to collect GNSS data at baseband (low Intermediate Frequency (IF)), which provided high resolution analysis of the carrier phase tracking data of both GPS and GLONASS modernized satellite signals, as a function of potential charge distributions or electromagnetic (EM) interference adjacent to the high voltage conductors.

1.3 Project Timeline

The timeline of the research project is shown in Figure 1. The timeline includes the initial planning of the field test operations, the execution of actual testing, in-field initial validation of the data collected, as well as the demarcation of final evaluation and report completion.

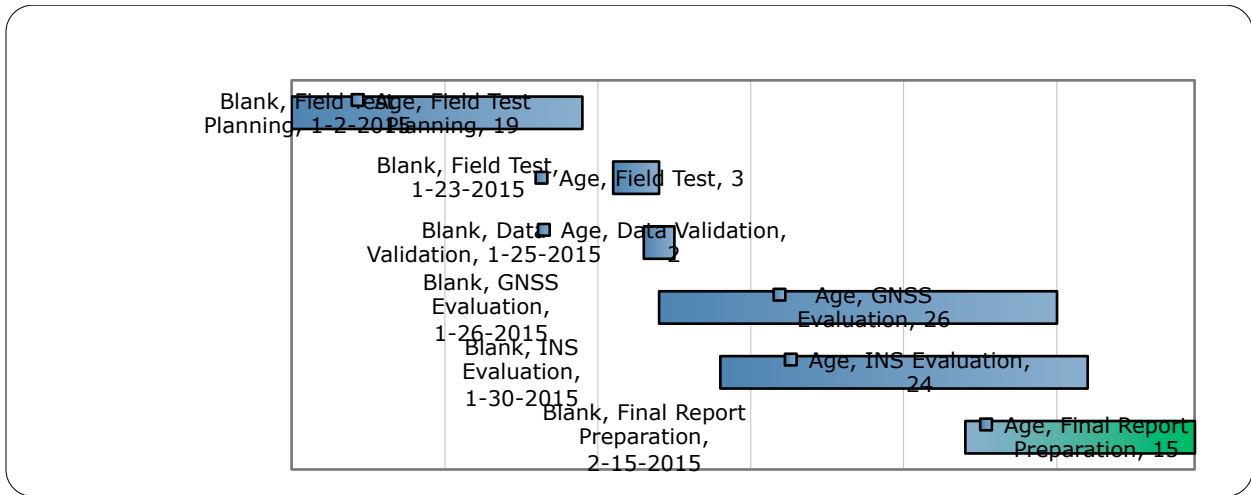


Figure 1 – Project timeline

2 Field Setup and Testing

2.1 Base Station Deployment

Base station deployment in support of differential data processing and real time kinematic (RTK) receiver testing was dictated by the testing profiles, the range of the Trimble R8 RTK system radio link, as well as the desire to maximize the distance between base stations and the potential effects of the power lines. In order to comply with the rated radio link limitation of 1 km while still allowing traversal testing under both DC bipoles as well as data collection parallel to and beneath multiple tower spans of the DC lines, the base stations shown in Figure 2 were deployed at the position indicated in Figure 3.



Figure 2 – Deployment of GNSS base stations on 24 January 2011. Novatel V3 receiver utilizes right tripod equipped with a Novatel 702-GG GPS+GLONASS L1+L2 antenna. Trimble R8 base unit occupies left tripod, with integrated receiver + antenna + radio module. Radio antenna is the black vertical bipole antenna visible under the R8 receiver body.

On the 2nd day of field data collection the deployment location of the base stations was transferred approximately 150 metres further west as the effective range of the radio link was found to be greater than the initial estimate.

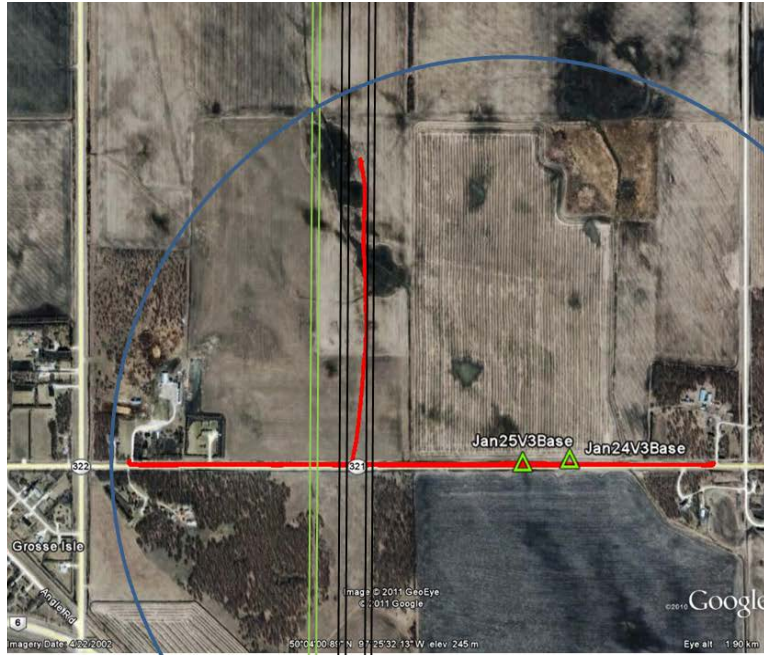


Figure 3 – Map of test location showing location of the V3 base stations for each day (green triangles), range of Trimble R8 450 MHz data link (blue circle), and position of DC bipole 1 and 2 (black lines), position of AC Line (green lines). Base map from Google (2011).

Data collected by the base stations included GPS and GLONASS pseudorange, carrier-phase, ephemeris and clock measurements. The Trimble R8 base station collected raw GNSS data and broadcasted corrections based on internal measurements and a temporary virtual point (the correct coordinates were determined after the data collection). The NovAtel V3 recorded all information to an internal memory card for later post-processing use. Serial numbers for all hardware used is provided in **Error! Reference source not found..**

2.2 Rover GNSS and HSGPS Deployment

Equipment supporting the mobile portion of the collection effort was divided between the roof of the test vehicle, depicted in Figure 4, and the cab of the truck where the operation of the navigation systems were monitored and managed.

Specific components of the test equipment installed on the vehicle roof were the Trimble R8 rover unit, the antenna for the high sensitivity GPS receiver, the NovAtel 702 GG pinwheel antenna used by the V3 mobile unit, the Novatel SPAN INS, and the PLAN

group Leapfrog-II L-Band Front-End module. The IMU component of the Novatel SPAN SE system was deployed on the roof of the vehicle to provide a rigid and stable mounting point via four magnets.



Figure 4 – Mobile GNSS, Inertial, and RF equipment elements mounted on roof of test vehicle. Trimble R8 rover unit at bottom right, high sensitivity GPS antennas on roof at right, Novatel 702 GG dome antenna centre left directly adjacent to LCI IMU (grey box) at centre left.

The block diagram of the complete navigation test system suite is shown in Figure 5.

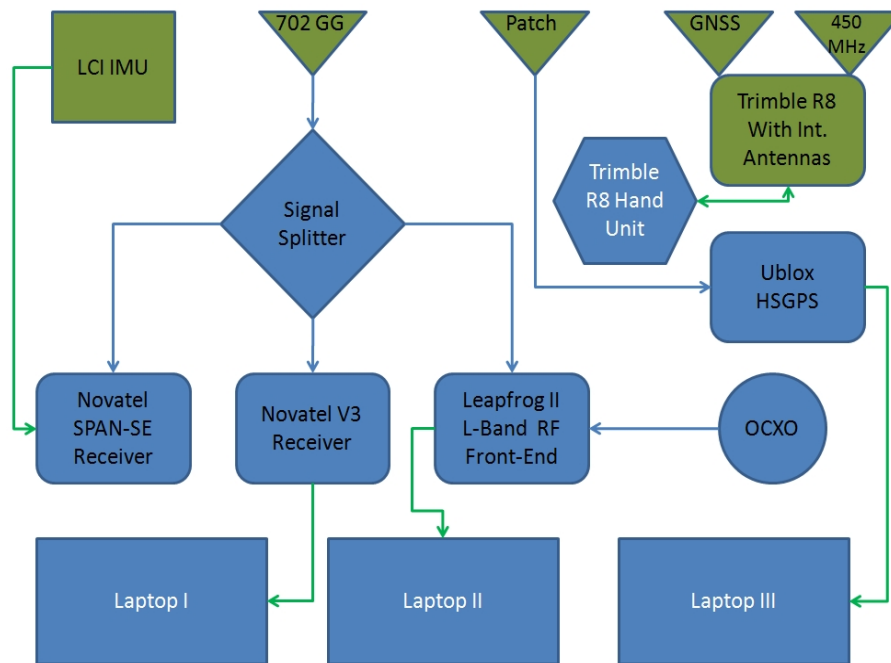


Figure 5 – Deployed equipment functional diagram. Equipment external to vehicle shown as olive green elements (antennas, IMU, Trimble R8), equipment installed inside vehicle shown in blue. Cabled RF links shown with blue arrows, digital data links shown with green arrows.

2.3 Reference INS Deployment

The use of the GNSS aided INS provided an independent reference solution that would still have operated in the presence of signal interference. An INS operates by measuring and integrating the accelerations and angular velocities to which it is subjected. Thus the IMU provides the relative position smoothing and GNSS provides the absolute navigation solution. The two observables (GNSS observations and IMU observations) are combined in a Kalman Filter where the biases of the IMU can be calibrated and removed.

Data was logged internally by the SPAN SE GNSS receiver. The SPAN SE receiver was configured to log all GPS and GLONASS data pertinent to post process a reference trajectory.

2.4 Rover RF Front-End Deployment

To provide an extra dimension of certainty to the testing results, the PLAN group Leapfrog-II L-band RF front-end was used to collect direct observations of the GNSS signals from both GPS and GLONASS satellites in the L1 and L2 navigation bands. By collecting and digitizing the microwave frequencies it was possible to post-process the data using the PLAN groups GSNRxTM software receiver (Petovello et al 2009) and provide extensive signal analysis capabilities not available from commercial hardware based receivers.

The primary observation goals of this equipment was to observe the potential effects of power line interference directly on the L-Band navigation signals as a function of the distance to power line dependent carrier to noise ratio degradation effects (if present), in addition to the potential observation of any deleterious effects which might be attributed to corona discharge directly adjacent to the high voltage lines themselves.

The origins and effects of corona discharge are described by Phillips (2007), Juette (1971) and Pacific Gas and Electric (2005). Previous work such as Juette (1971) has shown that interference is possible over a wide range of frequencies. For this reason one must consider the possibility that interference may be observed at even higher GNSS signal populated frequency bands.

To reliably observe any interference due to proximity to the high voltage DC bipoles, the data collected by the front-end will be analyzed via GSNRx™ to isolate any Carrier to Noise density deviations from expected values that would occur in the presence of interference to the L-Band GNSS navigation signals.

Additionally, the locally ionized atmosphere around the high voltage conductors as discussed by Pacific Gas and Electric (2005) could be superficially compared to the naturally occurring ionized atmosphere in the ionosphere. The effect of the ionosphere on the propagation of navigation satellite signals is directly observable when using multiple signals at different frequencies originating from the same satellite such as the L1 and L2 civil signals from GPS and GLONASS. This is due to the charged atmospheric layers being dispersive at L-Band frequencies, thereby imparting a varying signal delay effect inversely proportional to the square of the carrier frequency as discussed in Morrison (2010):

$$\Delta S_{iono,g} = \frac{40.3TEC}{f^2} \quad (1.1)$$

In equation (1.1) ΔS is the change in metres of the apparent signal path length, TEC (Total Electron Content) is the amount of charge encountered within a 1 m² column around the ray path of the signal where 10¹⁶ ions is 1 unit of TEC, and f is the carrier frequency of the signal. Since the GPS L1 carrier is located at 1575.42 MHz while the L2 carrier is located at 1227.6 MHz, this has the consequence of introducing a 16.2 cm per unit of TEC bias in the L1 range measurement and a 26.7 cm per unit of TEC bias in the L2 range measurement. The magnitude of the effect on the carrier phase is equal,

but the sign is reversed such that increasing levels of TEC appear to cause a decreasing range between the satellite and the user. By measuring the evolution of the difference between the L1 and L2 carrier phase observations it is possible to measure the changes in encountered charge with high certainty, as each TECU of charge increase or decrease will cause a phase difference magnitude change of 10.5 cm between the two carriers of a GPS satellite.

Conceptually, the local ionization of the atmosphere adjacent to the high voltage conductors could cause a similar effect, however the expected ion current density of 60 nA per square metre discussed in Lundkvist et al (2009) for a 500 kV DC line would be expected to produce a completely negligible effect on the order of microns. If one assumes that the peak referenced current density is uniform over a 1 metre vertical cross section between the bipole conductors, this would cause a GNSS signal passing through this region from directly above to encounter a charge of 60 nano Coulombs. Since one Coulomb is equivalent to 6.24×10^{18} elementary charges, the total encountered charge would be equivalent to 3.74×10^{11} elementary charges. In terms of the previously discussed units of TEC, this total encountered charge could be stated as 3.74×10^{-5} TECU. Since one TECU of encountered charge increase or decrease causes a 10.5 cm divergence between the L1 and L2 carrier measurements, the total encountered charge of 3.74×10^{-5} TECU would produce an expected carrier phase difference change of only 3.93 micrometres.

To validate the negligible nature of this effect, the Leapfrog-II front-end was used to collect observations from modernized (dual civil frequency) GPS and GLONASS satellites at high elevation angles. By using observations from high elevation angle satellites whose ray path would intersect the transmission lines and the charged air between them during a perpendicular crossing run of the lines, direct measurement of the effect of air ionization was made possible via the aforementioned differential L1 and L2 carrier propagation rates in charged atmosphere. The results of post processing these measurements are presented in Section 3.3.

3 Data Evaluation

Nineteen segments of data were selected from the two day collection period to show key indicators of GNSS quality in real time differential (and single point) positioning mode. Table 1 shows details of each test segment. The software processing strategies are summarized in Table 2. More information on the software is also provided in Appendix B.

Table 1 – Data Segment Information

Segment	Type of Segment	Heading	GPS Start Time (s)	GPS End Time (s)	Duration (s)	Average Speed (km/h)	Segment Distance (m)	Notes
Day 1 – Monday Jan 24, 2011								
**1	Perpendicular	West	152925	153030	105	15.4	448.7	
2	Perpendicular	East	153263	153476	213	15.6	456.0	Static Between 153288 - 153427 (139 s)
3	Perpendicular	West	153771	153843	72	22.3	448.6	
4	Perpendicular	East	154092	154172	80	20.2	448.6	
5	Perpendicular	West	154686	154810	124	13.2	453.6	
6	Perpendicular	East	155052	155184	132	12.5	451.3	
7	Static Under Lines		155675	156130	455	0.0	0.0	Under DC2 (middle) on road
8	Along Track	North/South	156580	157055	475	12.2	1441.4	
9	Along Track	North/South	157795	158229	434	13.5	1451.7	
Day 2 – Tuesday Jan 25, 2011								
10	Perpendicular	West	246003	246117	114	14.3	451.7	
11	Perpendicular	East	246342	246460	118	13.8	450.2	
12	Perpendicular	West	246863	246998	135	11.8	229.7	OEMV3 data stopped logging due to loose USB connection
13	Perpendicular	East	247225	247337	112	14.5	450.0	
*14	Perpendicular	West	247843	247965	122	13.3	450.4	
15	Perpendicular	East	248207	248312	105	15.8	459.1	
16	Static Under Lines		248777	248925	148	0.0	0.0	
17	Along Track	North/South	249025	249415	390	14.3	1449.0	
18	Along Track	North/	249596	250210	614	10.4	1436.1	GPS Antenna

		South						Fell Off, Static from 249703 - 249862 (159 s)
*19	Along Track	North/ South	250340	250887	547	10.2	1455.3	

* - Denotes analysis in Section 3.2 & 3.4

** - Denotes analysis in Section 3.3

Table 2 – Software Processing Strategies

Software	GNSS Data
NovAtel Inertial Explorer	IMU + L1+L2 GPS+GLONASS
University of Calgary’s PLANSoft™	L1 GPS+GLONASS
University of Calgary’s GSNRx™	L1+L2 GPS+GLONASS
NovAtel’s GrafNav	L1+L2 GPS
Trimble R8 Internal RTK Solution	L1+L2 GPS+GLONASS
U-blox Internal Solution	L1 HSGPS

3.1 Reference Solution Evaluation

An important step in any validation of a result is to ensure the reference trajectory is performing in a satisfactory manner. In comparing a fixed carrier phase ambiguity solution (as often used in precision agriculture commercial products), the reference trajectory must be comparable to the accuracy of a fixed ambiguity solution. Therefore, this section is included to show that the reference INS solutions provided an acceptable solution.

The differential GNSS mode was used and the data was processed in forward and reverse mode, smoothed using RTS (Gelb 1974) smoothing and finally combined to form the final reference trajectory. The software indicated that a fixed solution was used throughout the data collection.

Figure 6 shows the estimated standard deviations of the output positions on Jan 24 (the Jan 25 solutions have similar behavior). The position standard deviations are used as a “sanity check.” The estimated standard deviations indicate there were no issues

resulting from potential GNSS data outages that would hinder the solutions. Some occasional discontinuities are seen. These occur outside the test segments and are related to people working close to the antenna thereby resulting in signal shading, vehicle dynamics (the vehicle entering the ditch where it experienced a high pitch and moderate roll) and prolonged static times where the IMU biases are not as effectively estimated (i.e. IMU errors are more accurately estimated under dynamics).

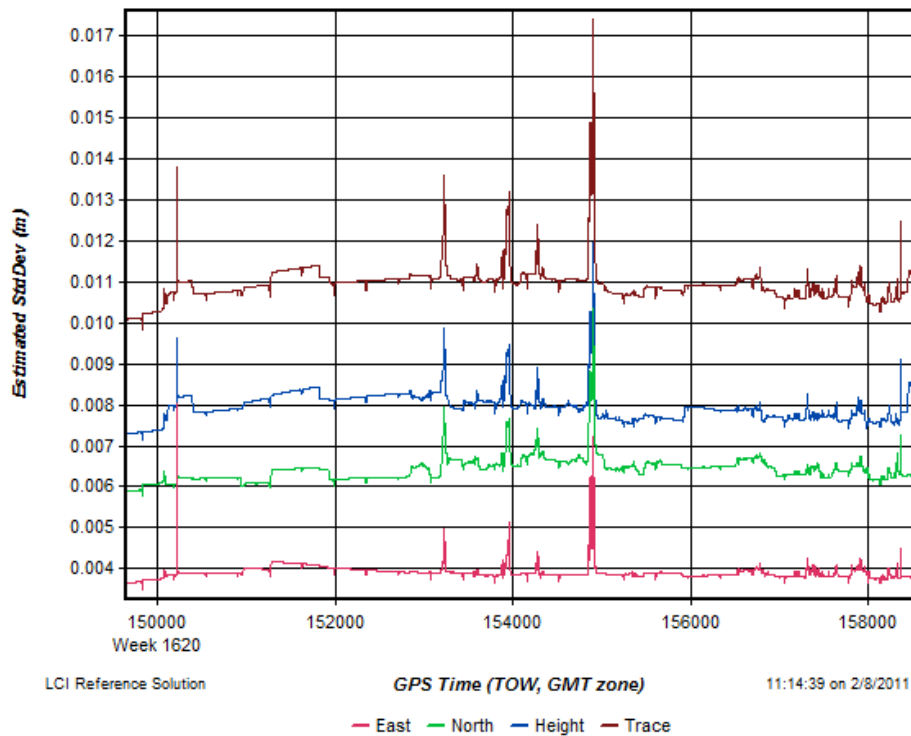


Figure 6 – Estimated Standard Deviation (1σ) of the Reference Trajectory as Output by Inertial Explorer

Figure 7 shows the differences between the estimated positions derived from the IMU and the GNSS solutions used to aid the INS. The positions derived from the IMU are computed by using the mechanization equations to convert from angular velocity and specific force to changes in orientation and position. Thus Figure 7 shows that the agreement between the IMU and GNSS navigation solution is extremely good, namely better than a few centimetres. The discontinuities that occur correspond to the standard deviation increases seen in Figure 6.

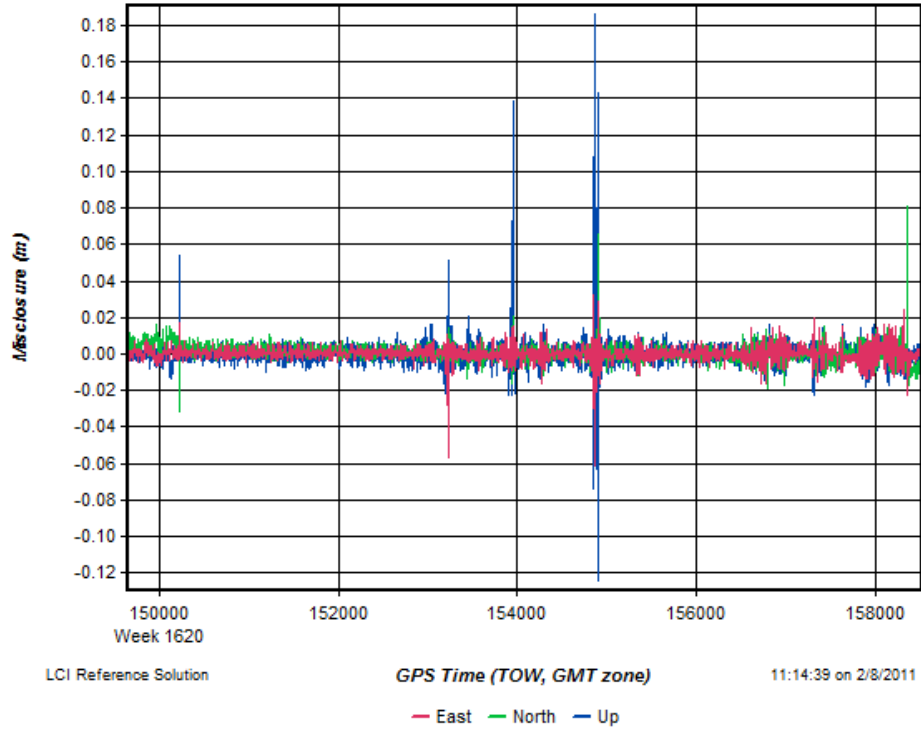


Figure 7 – Difference in IMU Mechanization Positions and GNSS Positions as Output by Inertial Explorer

3.2 Differential GNSS Observations

3.2.1 Trimble RTK Analysis

The position errors of the Trimble Real Time Kinematic (RTK) system are shown in Figure 8 and Figure 9 for segments 14 and 19, respectively. Discrepancies of several cm to 1 dm are common amongst receiver manufacturers and processing software, thus the errors shown on the top of Figure 8 are completely normal. The errors are a sum of antenna phase center variation (two systems), projection of the reference solution to the Trimble R8 antenna, carrier phase noise and multipath, and differences in filtering and estimation techniques used.

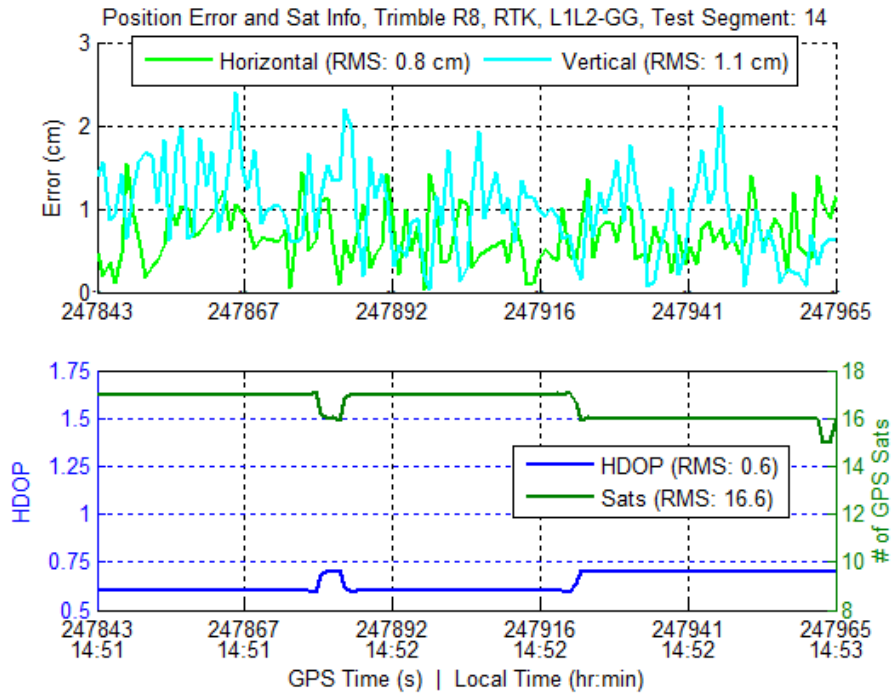


Figure 8 – Position Errors and Satellite Geometry, Receiver: Trimble R8, Processed by: Trimble Internal RTK Solution, Data: L1+L2+GPS+GLONASS, Test Segment: 14

The RTK solution of segment 19, as shown in Figure 9, contains errors upwards of 12 cm, with an RMS of 3.4 cm. Segment 19 is a north/south trajectory underneath the DC bipoles and was conducted on a snow covered semi-plowed field. These positions are derived from a float solution, in which case the carrier phase ambiguities are estimated as stochastic quantities. This often used technique results in lower accuracies (of several decimetres). These errors are consistent for all North/South segments (segments 17 - 19) where the vehicle was on uneven paths. A fixed solution was maintained when the vehicle was on the paved road with minimal dynamics. During the static section of segment 18, the RTK solution was then able to fix and provide results similar to those of the perpendicular and static tests (see Figure A97). Further, the GrafNav solution, shown in Figure 11, was able to fix the ambiguities, indicating that the GNSS measurements are good and of the quality expected under line-of-sight conditions.

In regards to segments 17 – 19, there are a few contributing factors that would yield a float solution instead of a fixed solution, namely (i) the GNSS measurement quality

(excessive noise or multipath), (ii) failure or weakness in the RTK data link and (iii) the algorithm/software used to determine the ambiguity. The first potential factor was eliminated by showing that the GNSS measurement quality is normal through post-mission processing. It is not possible to fully verify (iii) due to the proprietary nature of the receiver algorithms/software implemented to fix the ambiguities. It is not possible either to verify (ii) as there is no information on the number of data packets or checksums lost in the data link. Thus, because a fixed solution was possible by processing the measurements in post-mission with GrafNav, it is only possible to confirm that the GNSS measurements were not at fault in the float solution of the Trimble RTK solution. The uneven path of section 17 – 19 (in addition to 8 and 9) resulted in vibrations and jerks in the antennas. This may have affected the quality of the data link. As explained above, it is not possible to fully verify this due to the lack of data link measurement checks available to the user. As to whether the Trimble data link performance might have been directly affected by the overhead power lines during the along-track tests but not during perpendicular tests cannot be confirmed or denied due to the lack of evidence.

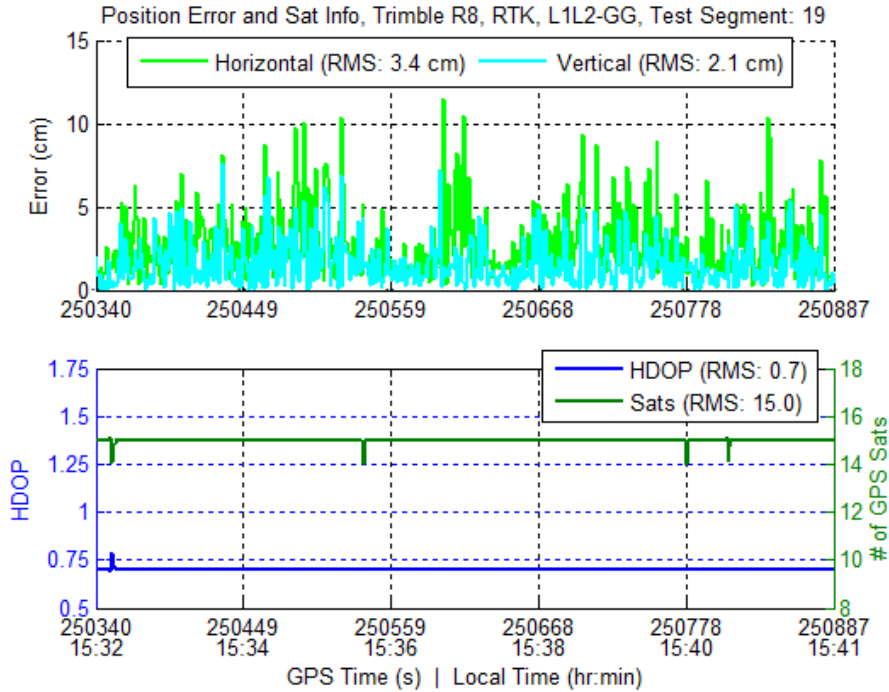


Figure 9 – Position Error and Satellite Geometry, Receiver: Trimble R8, Processed by: Trimble Internal RTK Solution, Data: L1+L2+GPS+GLONASS, Test Segment: 19

Referring back to the two previous figures, the HDOP and number of satellites presented in the bottom half of Figure 8 and Figure 9 are consistent with expected open sky conditions. The solution of the RTK system may, for example, reject a satellite without a fixed ambiguity, occlude some satellites near the horizon or have difficulty maintaining signal lock for a low elevation satellite. The values presented in Figure 8 and Figure 9 show ideal data, with no reason to yield navigation impediments. A HDOP of 0.6 is among the best values currently available with a GPS+GLONASS receiver at the latitude of the tests.

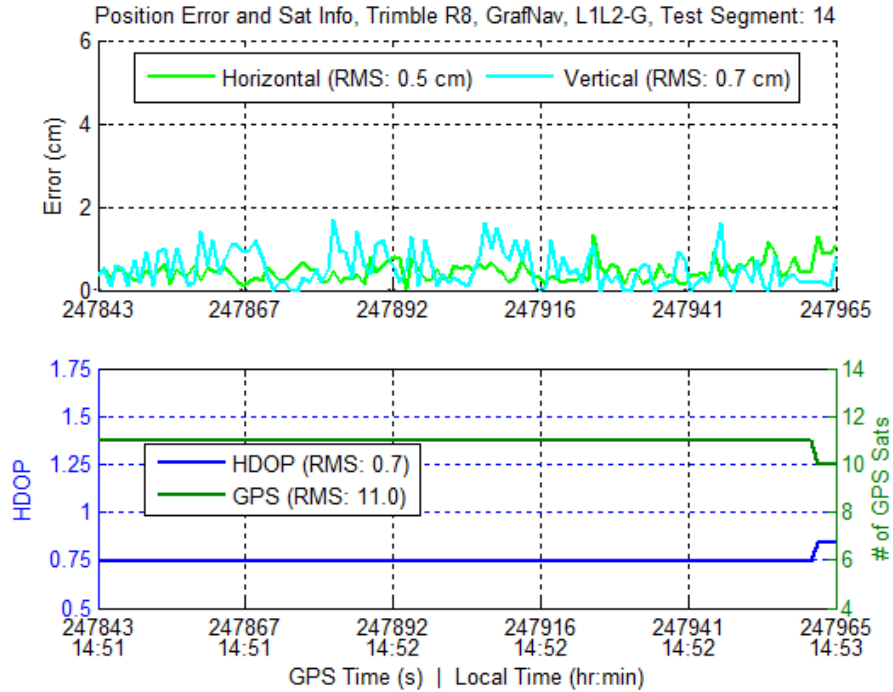


Figure 10 – Position Errors and Satellite Geometry, Receiver: Trimble R8, Processed by: NovAtel’s GrafNav, Data: L1+L2+GPS, Test Segment: 14

The RMS error of Segment 19, shown in Figure 11, for the GrafNav solution is 0.8 cm larger than the perpendicular case (0.5 vs. 1.3 cm). This is attributed to carrier phase multipath and noise, the dynamics experienced by the vehicle and the ability to map the reference solution to the Trimble R8 antenna phase center. The number of satellites and HDOP of the solution were still excellent.

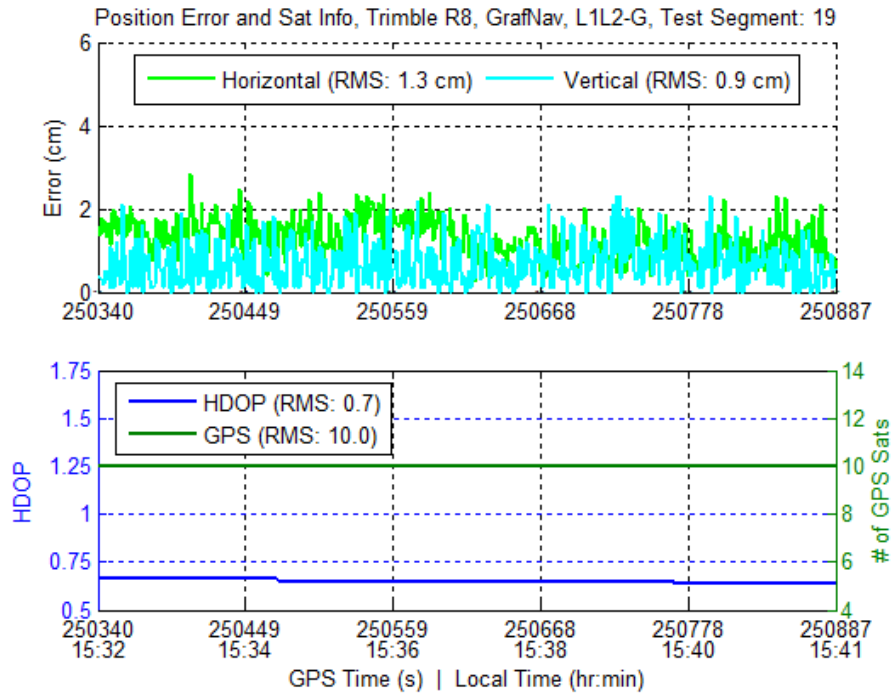


Figure 11 – Position Error and Satellite Geometry, Receiver: Trimble R8, Processed by: NovAtel’s GrafNav, Data: L1+L2+GPS, Test Segment: 19

3.2.2 NovAtel Receiver Analysis

The NovAtel receiver and PLANSoft™ software combination represents a second and independent system to assess performance under power lines. This section will analyze receiver and software performance for the same segments as previously, namely 14 and 19.

3.2.2.1 Received Signal Power

Figure 12 and Figure 13 show the average carrier to noise density (C/N_0) for all satellites tracked by the receiver for segments 14 and 19. The results are comparable to those of open sky data and no evidence of power line disturbances is present. L2 signals are broadcasted at 1.5 dB lower power (IS-GPS-200E 2010) than L1 and the 702GG antenna gain pattern amplifies the L2 signal 3 dB less than the L1 signal at zenith (NovAtel Inc. 2010).

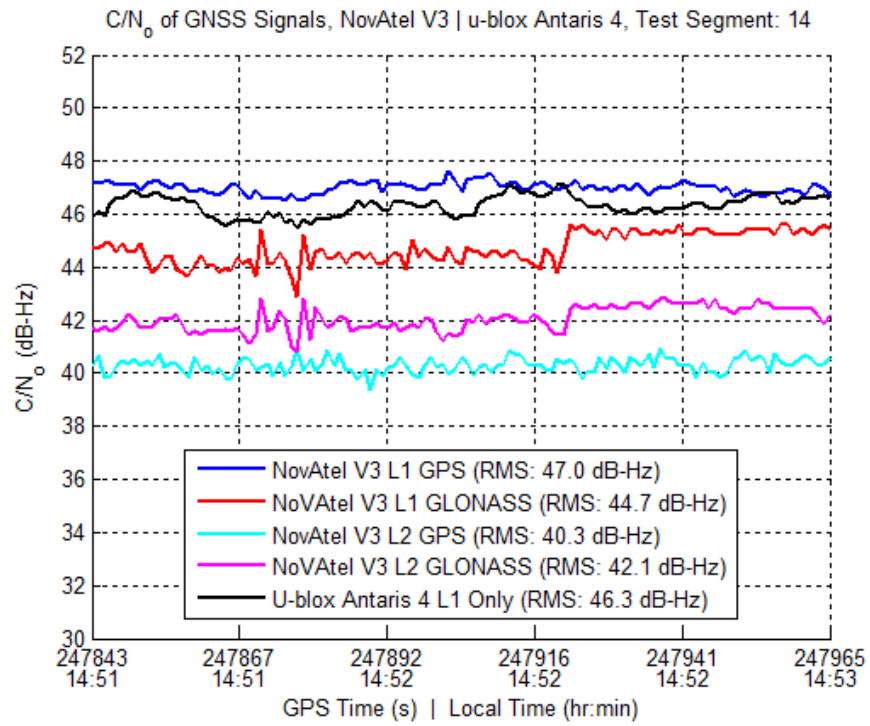


Figure 12 – GNSS Signal Strength, Receiver: NovAtel V3, Data: L1+L2+GPS+GLONASS, Test Segment: 14

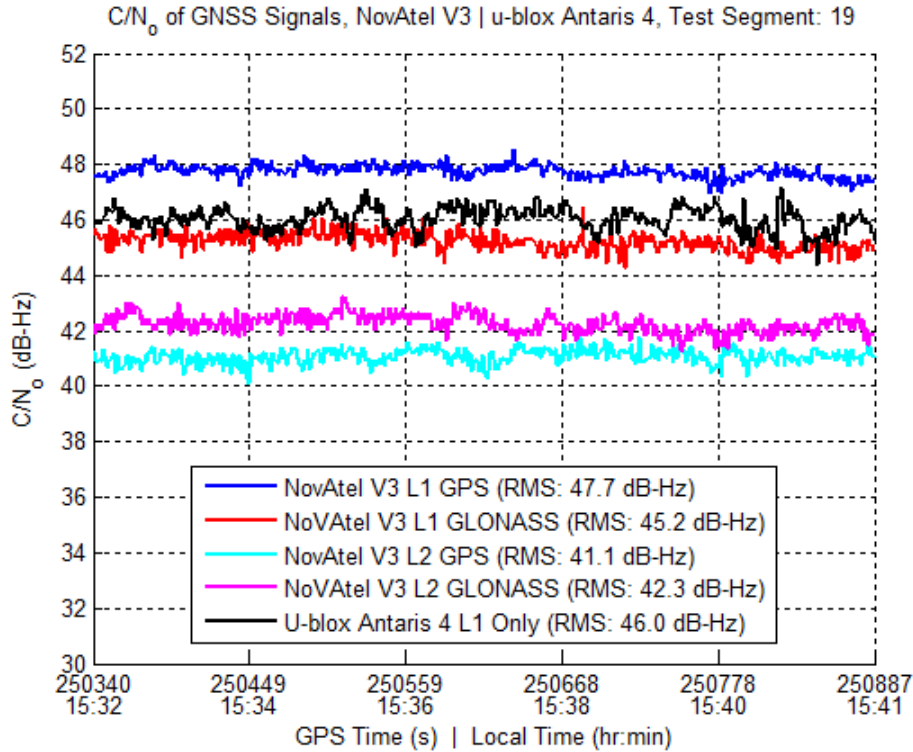


Figure 13 – GNSS Signal Strength, Receiver: NovAtel V3, Data: L1+L2+GPS+GLONASS, Test Segment: 19

3.2.2.2 Position Errors and Satellite Geometry

Similar to the Trimble RTK solution, position errors and satellite geometry plots were generated for all segments and are available in Appendix C. Segments 14 and 19 as processed by PLANSoft™ are shown in Figure 14 and Figure 15. Both segments exhibit errors less than 1 cm as compared to the reference trajectory. The HDOP is exceptional throughout both segments and the number of satellites remains consistent with open sky conditions. No power line effect is detected.

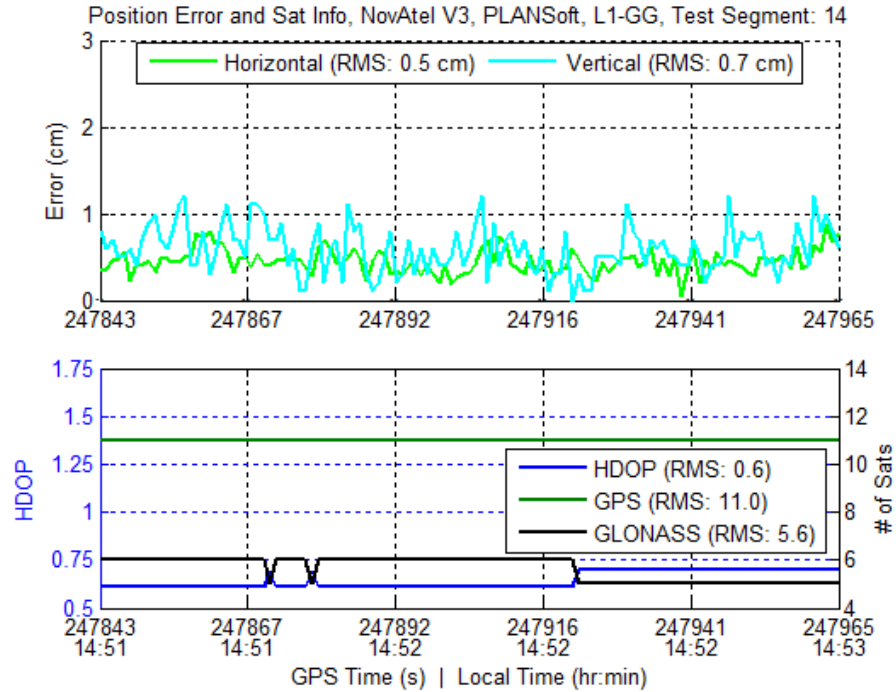


Figure 14 – Position Error and Satellite Geometry, Receiver: NovAtel V3, Processed by: PLANSof, Data: L1+GPS+GLONASS, Test Segment: 14

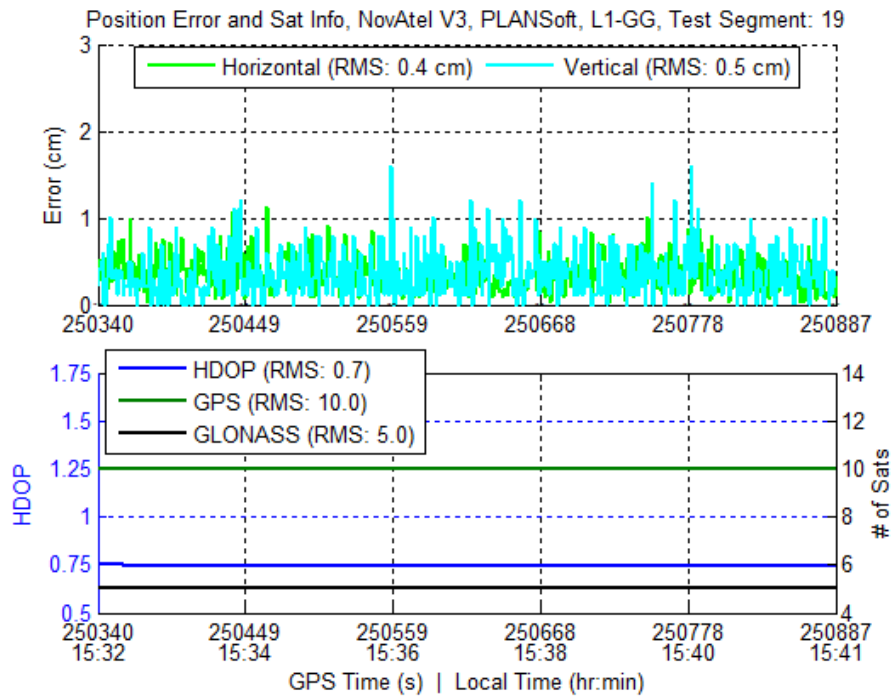


Figure 15 – Position Error and Satellite Geometry, Receiver: NovAtel V3, Processed by: PLANSof, Data: L1+GPS+GLONASS, Test Segment: 19

3.2.2.3 Residual Errors

PLANSofTM outputs the residual error (referred to as a residual in the sequel) of each measurement used in the filter that can then be used to validate the solution. A residual is the difference between the measured (or observed) value and the corrected measurement after all the data has been fused together to form the final and unique solution. Thus, small residuals indicate that the measurements are consistent with each other. There are additional factors that contribute to larger residuals, namely (i) noise and (ii) other errors in the measurement model. For instance, errors due to power line effects would result in higher residuals.

Figure 16 and Figure 17 shows the RMS of the residuals for all measurements used within an epoch. Measurements that might be rejected by the fault detection algorithm within the software are not used in the computation of the residual RMS. There was a minimal rejection rate in each data set, a common occurrence among GNSS data gathered under open sky conditions. For example, on Jan 24th there was a 0.067 % rejection rate of GPS and GLONASS observations. The rejection rate was therefore not higher than normal due to operation under the power lines. Code residuals of 0.5 m and less are exceptional and indicate quality observations with no hindrances. Phase residuals are also excellent at less than 1 cm. Given the number of satellites used, it is clear from this residual analysis that the receiver is functioning normally and with no effect from the power lines.

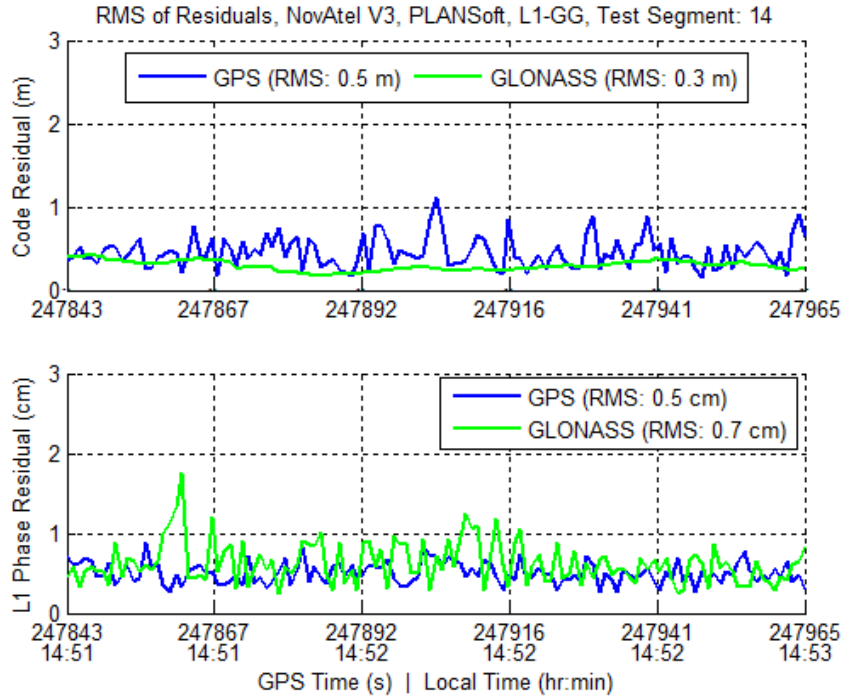


Figure 16 – RMS of Residuals, Receiver: NovAtel V3, Processed by: PLANSofT, Data: L1+GPS+GLONASS, Test Segment: 14

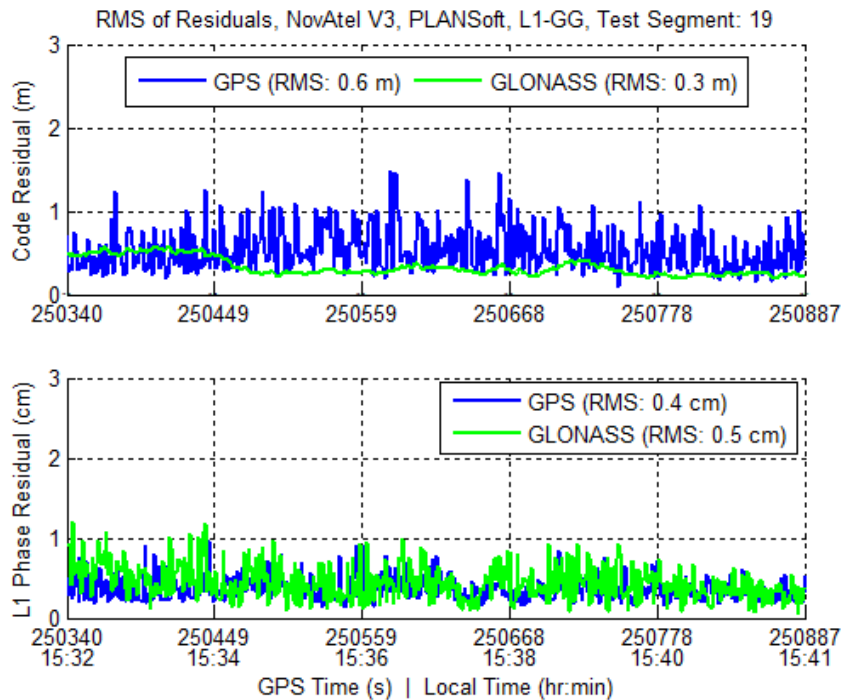


Figure 17 – RMS of Residuals, Receiver: NovAtel V3, Processed by: PLANSofT, Data: L1+GPS+GLONASS, Test Segment: 19

3.2.3 Carrier Phase Cycle Slip Analysis

Carrier phase cycle slips occur when the receiver loses carrier phase lock on the signals. This is commonly experienced when an obstruction blocks the direct line of sight to the signals, in which case the ambiguities affected must be reinitialized in the navigation solution. When one satellite experiences a cycle slip, the navigation filter can typically re-estimate the ambiguity within a few measurement epochs. However, if cycle slips occur on all channels simultaneously, such as when an antenna passes under an overpass, the entire ambiguity resolution process takes much longer to fix, degrading the navigation solution accuracy in the process. Thus, the number, frequency and location of cycle slips are important metrics to analyze as they affect the navigation solution quality.

Figure 18 shows the trajectories traveled during the data collection and each cycle slip is plotted on the trajectory. Numerous cycle slips occur on the east and west ends. This is due to the trees present on either side of the road, and low elevation satellites affected by these trees experience a large number of cycle slips. This is normal and to be expected. Some slips occur just east of the north/south trajectory where trees are present south of the road. Most importantly, although a few cycle slips occur under the lines, there is only a weak correlation between the location of the power line towers and the location of the cycle slips. This indicates that the power lines (and their corresponding towers), regardless of their electric current carrying characteristics, are not causing cycle slips at a level that would impede precision navigation.



Figure 18 – Geo-Located Cycle Slips (red: 24 Jan, purple: 25 Jan), blue rectangles indicate Figure 19, Figure 20 and Figure 21

Figure 19 through Figure 21 shows close up views of Figure 18. Figure 19 shows that when passing the towers (which appear on the map as dark circular areas), there are only a few cycle slips and their frequency is minor in comparison to that of those observed near the trees in Figure 21. It is also noteworthy that, despite a tower being located a few tens of metres from the northern most point of the data collection (where the vehicle turned to return south), no cycle slips were recorded in this area, further confirming the low effects of power line towers on carrier phase measurements.

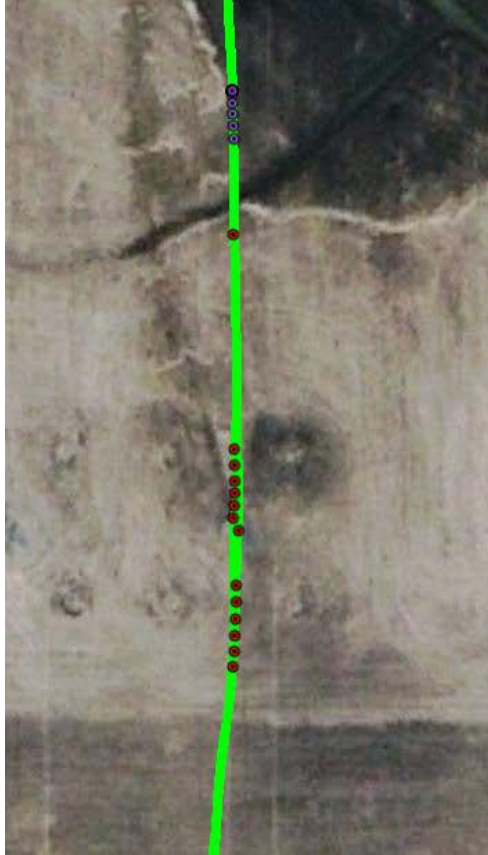


Figure 19 – Geo-Located Cycle Slips (red: 24 Jan, purple: 25 Jan)

Figure 20 shows the bipole towers and few correlated cycle slips in proximity of the power lines and towers.

It should be noted that the figures presented in this section contain all the NovAtel data collected, not just the segments analyzed (e.g. segments 1-19). This was to show the impact of trees on cycle slips versus the lines and towers overhead.



Figure 20 – Geo-Located Cycle Slips (red: 24 Jan, purple: 25 Jan)

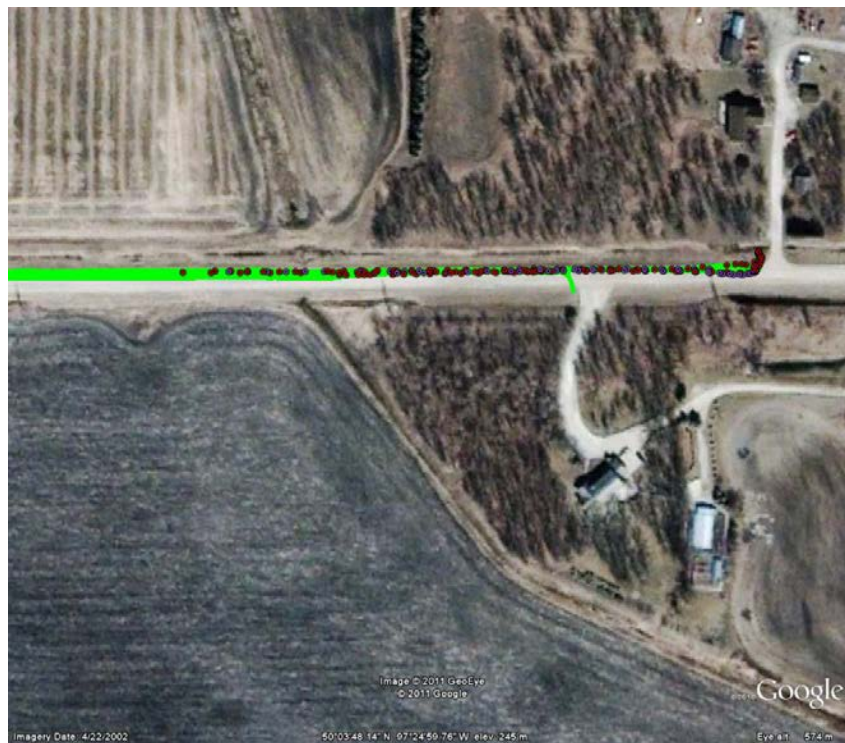


Figure 21 – Geo-Located Cycle Slips (red: 24 Jan, purple: 25 Jan)

3.3 RF Front-End Measurement Analysis

As discussed in Section 2.4 the measurements obtained from the RF front-end can be used to derive L1-L2 carrier divergences that would occur if the air ionization from the power lines was far stronger than predicted, as well as signal strength fading effects that would be observable if the power lines were emitting interference in the L1 or L2 bands.

If air ionization effects were present, they would be observed as a change in the L1 minus L2 carrier phase observations as the ray path between the satellite and the user traversed the conductors of the power line, as well as the region between the conductors. If interference was emitted from the power lines, it would be observable as a decrease in the carrier-to-noise density ratio as the test vehicle approached the power lines, returning to normal as the vehicle passed to the other side of the transmission corridor. Since these effects would be most clearly discernable during a perpendicular test scenario, these results are presented first, starting with the observations from test segment 1, presented for three different satellites in Figure 22 , Figure 23 and Figure 24.

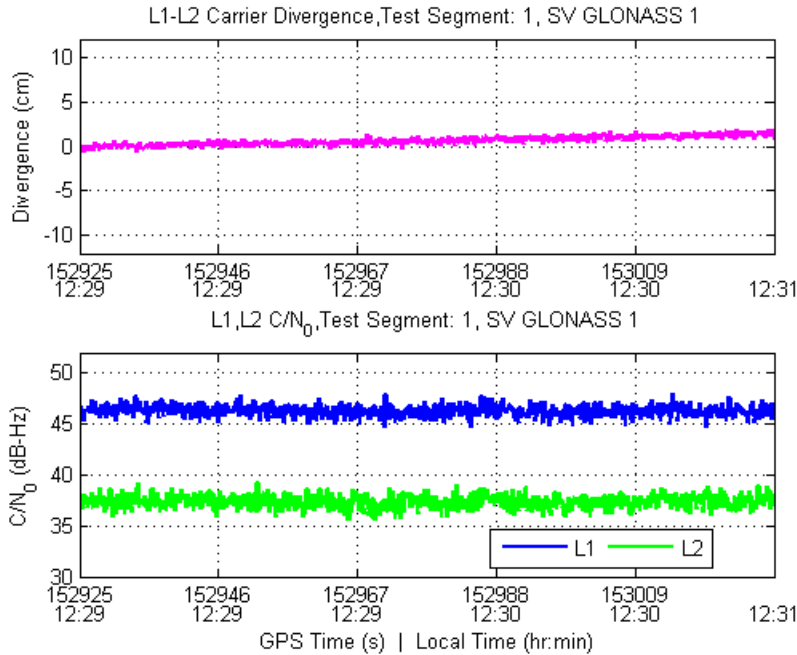


Figure 22 – Test segment 1 perpendicular crossing of power line corridor effect of two DC bipoles and 1 AC transmission line set on L1-L2 phase difference and carrier-to-noise density ratios of GLONASS M satellite in orbital slot 1. Lower L2 signal strength is due to lower transmitted signal strength from satellite in this band relative to L1 and lower gain of 702 GG antenna element at L2 frequencies. Traversal of eastern bipole centreline occurred at approximately 152962 seconds. Trend in carrier divergence is due to slowly changing ionospheric background conditions during test and is expected.

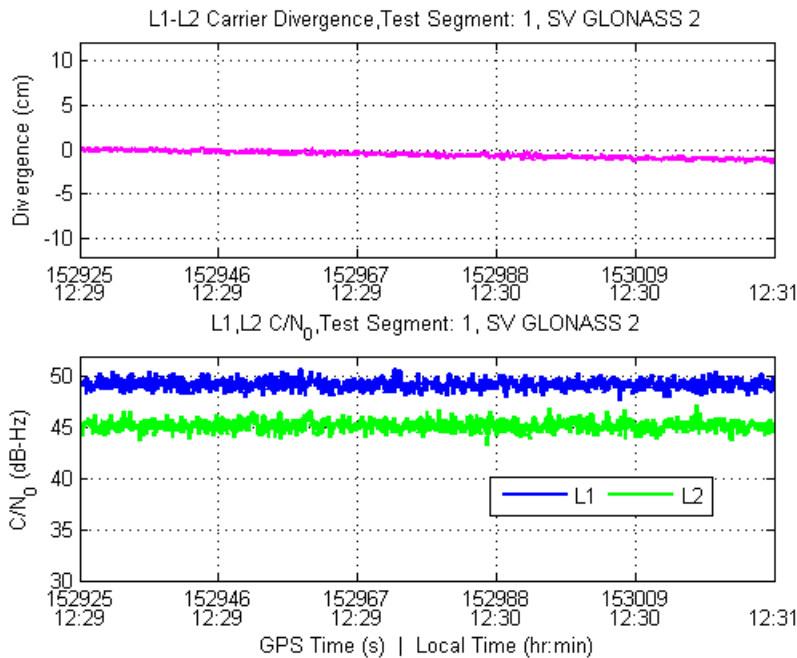


Figure 23 – Test segment 1 perpendicular crossing of power line corridor effect of two DC bipoles and 1 AC transmission line set on L1-L2 phase difference and carrier-to-noise density ratios of

GLONASS M satellite in orbital slot 2. Lower L2 signal strength is due to lower transmitted signal strength from satellite in this band relative to L1 and lower gain of 702 GG antenna element at L2 frequencies. Traversal of eastern bipole centreline occurred at approximately 152962 seconds. Trend in carrier divergence is due to slowly changing ionospheric background conditions during test and is expected.

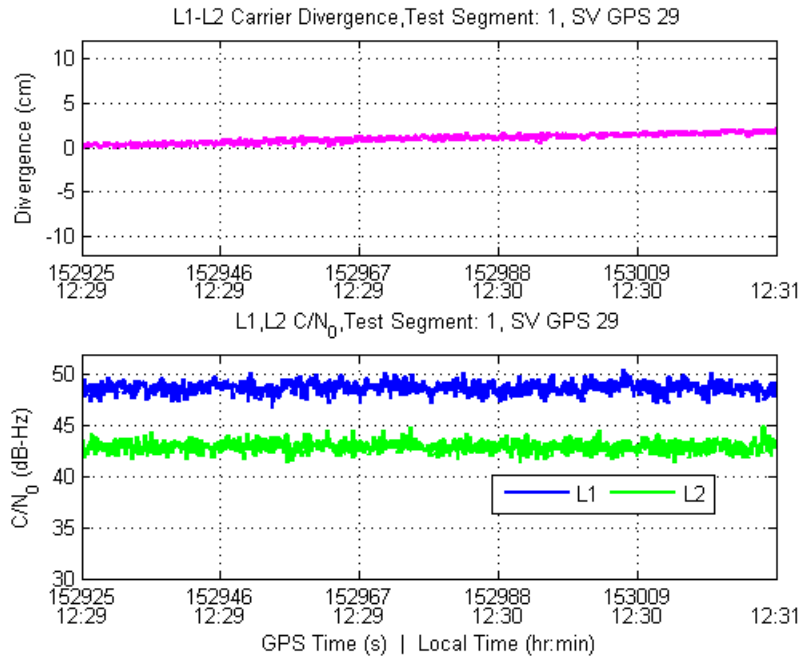


Figure 24 – Test segment 1 perpendicular crossing of power line corridor effect of two DC bipoles and 1 AC transmission line set on L1-L2 phase difference and carrier-to-noise density ratios of GPS IIR-M satellite transmitting PRN code 29. Lower L2 signal strength is due to lower transmitted signal strength from satellite in this band relative to L1 and lower gain of 702 GG antenna element at L2 frequencies. Traversal of eastern bipole centreline occurred at approximately 152962 seconds. Trend in carrier divergence is due to slowly changing ionospheric background conditions during test and is expected.

The signal characteristics presented in test segment 1 indicate no abnormal characteristics. No detectable RF interference is present in the GNSS navigation bands as evidenced by the nearly constant carrier signal strengths that show no noticeable reduction near the transmission lines. Additionally, the very slowly and smoothly varying carrier divergence measurement is indicative of normal background ionospheric effects, and shows no indication of a measurable effect due to air ionization adjacent to the transmission lines.

All perpendicular test trajectories produced similar null observations to those in Figure 22 through Figure 24. The results of all other perpendicular tests are contained in Appendix C, in Figure A106 through Figure A133.

Moving to the consideration of the carrier divergence and signal strength indicators produced during trajectories parallel to the power lines, deleterious effects were encountered, however these are the result of mundane signal blockage or antenna gain pattern variation such as the high vehicle dynamics requiring a 50% increase in GSNRx™ PLL bandwidth which causes a slight degradation of measurement quality, as well as the deep fades typically associated with solid objects such as trees intersecting the ray path between a low elevation satellite and the user antenna, and not due to interference from the power lines themselves.

As previously discussed in Section 2.4, the absence of any detectable effect on the GNSS navigation signals which is not explained by multipath or blockage is consistent with expectations. The trajectories taken parallel to the power line conductors did present challenges to the continuous tracking of some signals, but for reasons unrelated to interference or air charge distributions. These are now considered.

The results of the tests parallel to the conductors from the first day of field tests, specifically segments 8 and 9, are shown in Figure 25 through Figure 30.

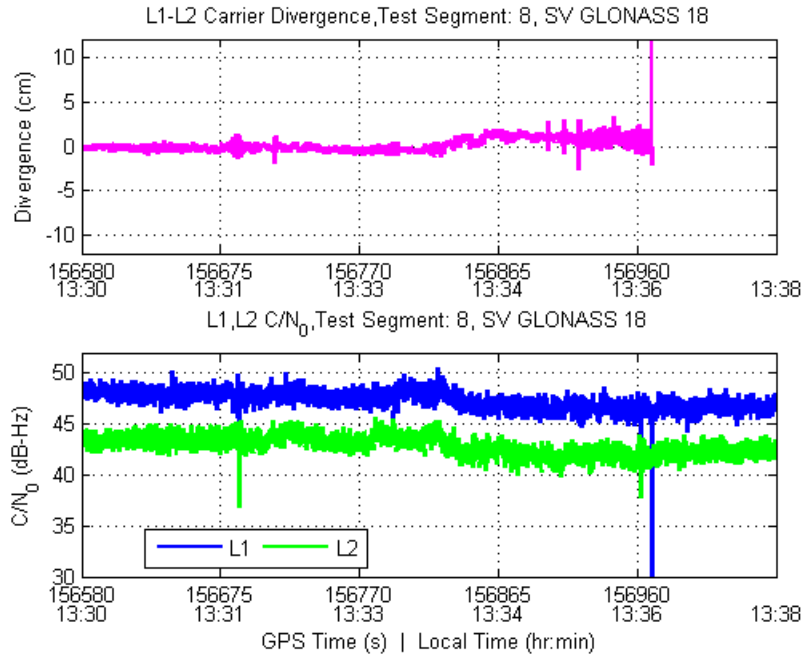


Figure 25 – Test Segment 8, parallel travel along transmission line corridor indicating brief blockage due to transmission towers on GLONASS SV 18. Deep fade on L1 results in multiple cycle slips causing off scale L1-L2 carrier difference, which is an expected result during signal blockage.

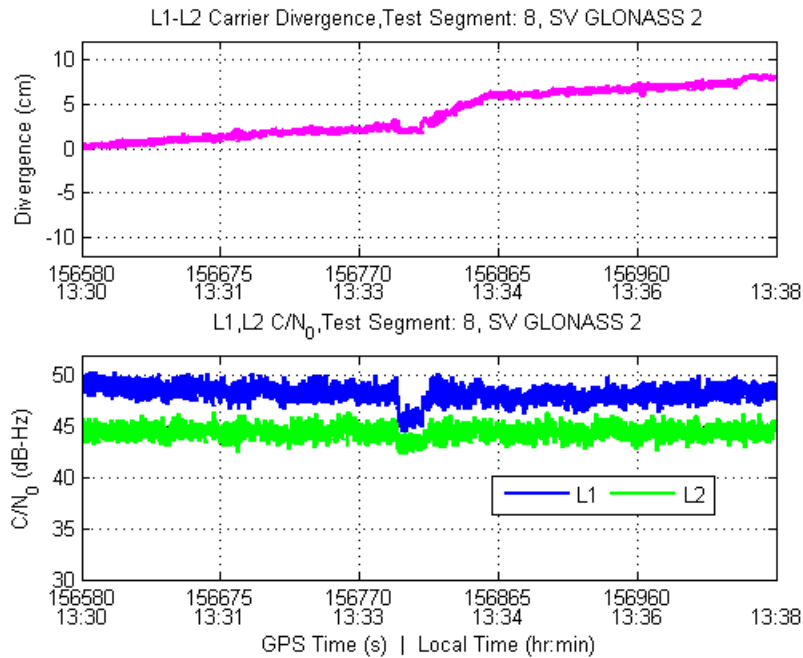


Figure 26 – Test Segment 8, parallel travel along transmission line corridor indicating brief blockage due to transmission towers on GLONASS SV 2. Shallow fade on L1 results in no cycle slip.

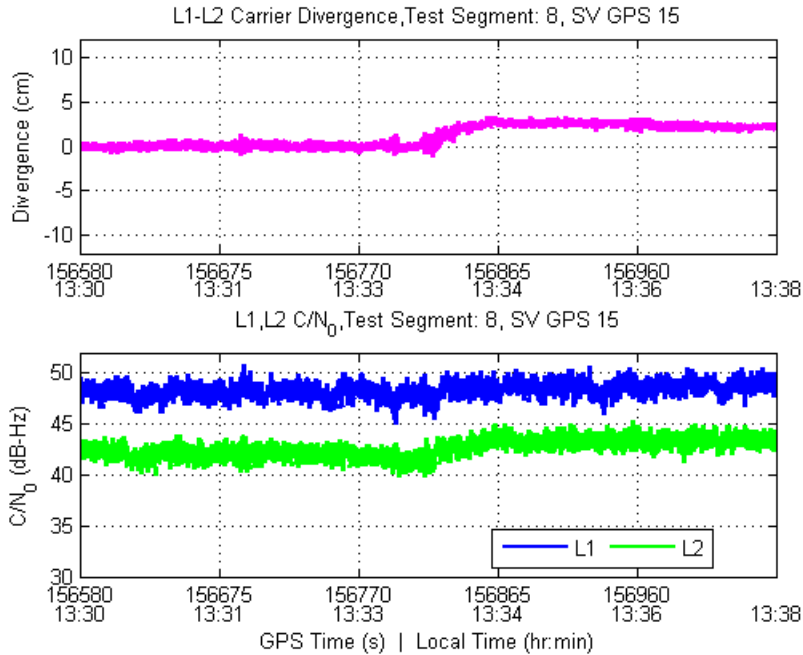


Figure 27 – Test Segment 8, parallel travel along transmission line corridor indicating brief blockage due to transmission towers on GPS PRN 15. No cycle slip occurrence.

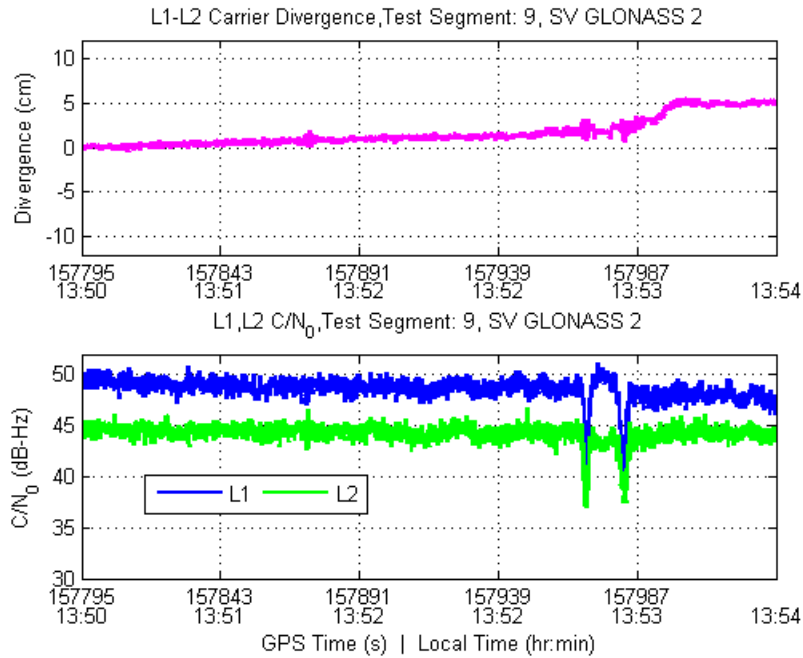


Figure 28 – Test Segment 9, parallel travel along transmission line corridor indicating two brief blockages due to transmission towers on GLONASS SV 2. No cycle slip occurrence

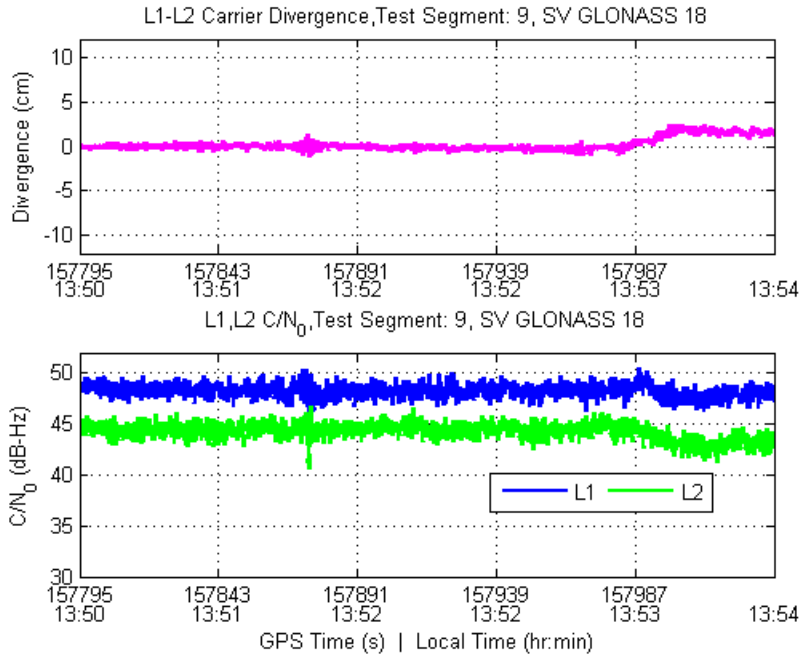


Figure 29 – Test Segment 9, parallel travel along transmission line corridor indicating brief blockage of L2 signal path on GLONASS SV 18. Apparent decrease in carrier strength in both L1 and L2 signals during final static portion of test believed to be due to change in inclination of GNSS antenna. No cycle slip occurrence

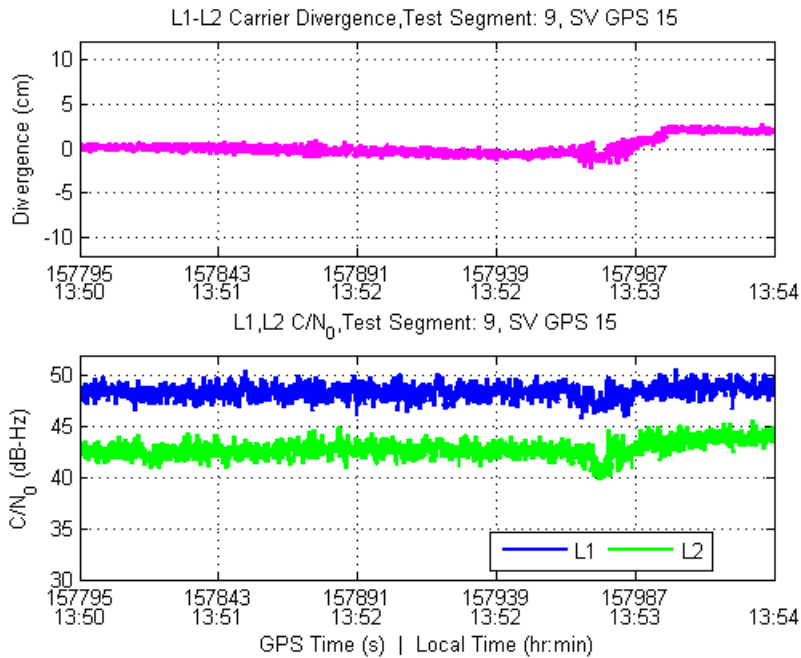


Figure 30 – Test Segment 9, parallel travel along transmission line corridor indicating brief blockage of L2 signal path on GPS PRN 158. Apparent increase in carrier strength in both L1 and L2 signals during final static portion of test believed to be due to change in inclination of GNSS antenna, increasing directional gain towards SV. No cycle slip occurrence.

Effects observed during the parallel motion segments 8 and 9 included changes in observed signal strength due to varying vehicle orientation, short deep fading due to blockage or multipath effects of the transmission towers, and some cycle slips as a consequence in a few instances. At no point however were consistent signal strength degradations noted simultaneously on multiple satellites that would indicate locally generated interference in the L bands.

Consistent changes in the carrier divergence of all satellites observed during parallel traversal tests are due to a phenomenon known as 'carrier phase wind up'. Due to the circular polarization of GPS and GLONASS signals, rotation of the receiving antenna results in apparent carrier phase advance or retreat from the point of reception. In the case of the testing executed, the windup effect is due to one half of a left turn at the far point in each trajectory where the direction of the truck is reversed from north facing to south facing. This negative one half-cycle is equivalent to a phase observed range change of -9.75 cm of GPS L1 signal phase, and approximately -12.2 cm of GPS L2 phase. The theoretical L1-L2 difference as a result of the left turn would therefore be predicted as +2.45 cm of divergence, which appears to precisely match the observed change.

Results of parallel traversal tests conducted on 25 January 2011 (segments 17 through 19) are included in Appendix C.

3.4 HSGPS Observations

High Sensitivity GPS is not typically used in precision agriculture applications. However, the HSGPS receiver tested herein was not hindered and suffered no additional errors other than would be expected by a single point GPS L1 only solution. Figure 31 and Figure 32 show the internal solution position accuracy and satellite geometry for segments 12 and 19, respectively. In general, the single point navigation solution should be within a few metres, and these results are no exception. In segment 14, 12 satellites were tracked continuously and the HDOP was 0.8, which is extremely good for a GPS only receiver. No dropouts occurred during either segment.

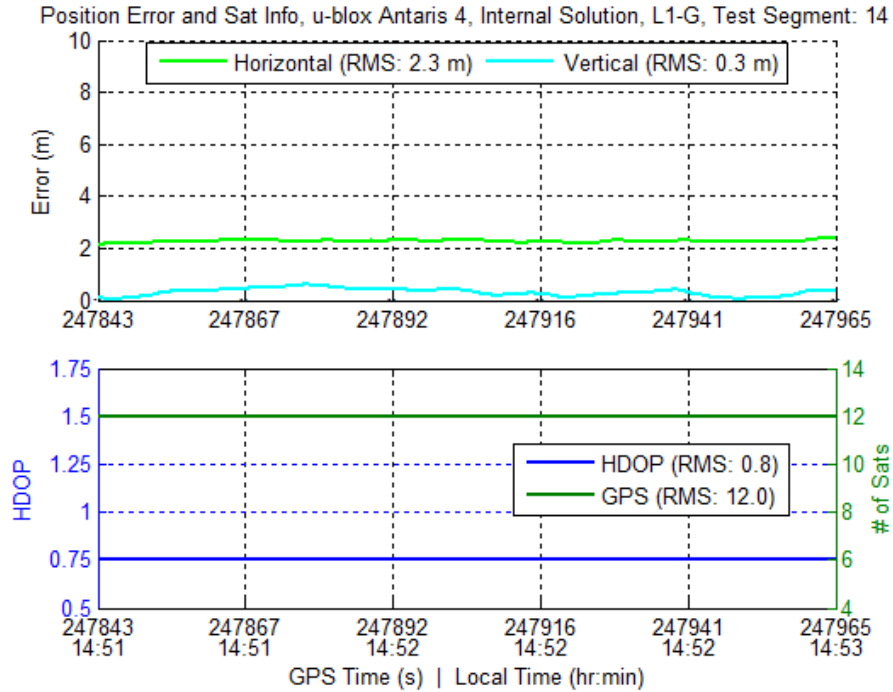


Figure 31 – Position Error and Satellite Geometry, Receiver: U-blox Antaris 4, Processed by: U-blox Internal Solution, Data: L1+HSGPS, Test Segment: 14

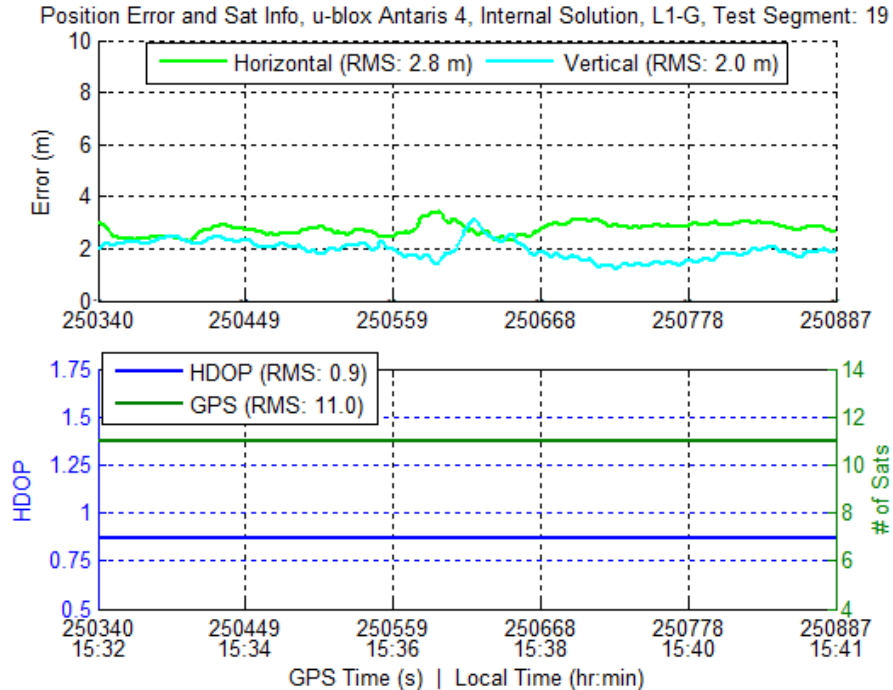


Figure 32 – Position Error and Satellite Geometry, Receiver: U-blox Antaris 4, Processed by: U-blox Internal Solution, Data: L1+HSGPS, Test Segment: 19

While not plotted, the u-blox Antaris 4 High Sensitivity GPS (HSGPS) receiver recorded similar power levels as that of the survey grade receivers, as expected. Variations are expected based on the Low Noise Amplifier (LNA) and gain pattern of each antenna.

4 Conclusions

This report analyzed GNSS data collected under two high voltage DC bipole lines. Using two survey grade GNSS receivers, a software based receiver, and a High Sensitivity GPS receiver, only minor adverse effects could be measured or observed due to the power lines or their respective towers. This report analyzed the following metrics to form this conclusion:

1. Position Accuracy
2. HDOP
3. Number of Satellites
4. RMS of Code and Phase Residual errors
5. Location and Number of Cycle Slips
6. Carrier to Noise Density (and Average of all Satellites)
7. L1-L2 Carrier Divergence

No power line effect on GNSS measurements was found to affect the quality of the navigation solutions.

In addition, the test results showed normal operation of a commercially available survey grade RTK system and its radio link (450 MHz) for static and perpendicular test segments perpendicular to the power lines. Four different processing packages (GSNRx™, GrafNav, PLANSoft™, and the Trimble RTK solution) were able to provide consistent results (with the exception of the RTK solution which was not able to provide a real time fixed solution when the vehicle experienced high dynamics when driving off road). No adverse effects were measurable in the IF data as processed by GSNRx™.

Other minor effects within the data were observed, but were not attributed to the overhead power lines or towers. These most likely resulted from high vehicle dynamics while driving off road, carrier phase wind up and cycle slips resulting from nearby trees.

5 References

Gelb, A. (1974) "*Applied Optimal Estimation*," The Massachusetts Institute of Technology Press.

IS-GPS-200E (2010) "Navstar GPS Space Segment/Navigation User Interface."

Juette, G.W. (1971) "Evaluation of Television Interference from High-Voltage Transmission Lines," *IEEE Summer Meeting and International Symposium on High Power Testing*, Portland, OR, pp. 4.

Lundkvist, J., I. Gutman and L. Weimers (2009) "Feasibility study for converting 380 kV AC lines to hybrid AC / DC lines," *EPRI's High-Voltage Direct Current & Flexible AC Transmission Systems Conference*, Westminster, CO, pp. 11.

Morrison, A. (2010) "*High Latitude Ionospheric Scintillation: Detection and Isolation from Oscillator Phase Noise as Applied to GNSS*," Ph.D. Thesis, Department of Geomatics University of Calgary, Canada.

NovAtel Inc. (2010) "*NovAtel GPS 702 GG Antenna Data Sheet*," pp. 2.

Pacific Gas and Electric (2005) " *Pacific Gas and Electric Delta Distribution Planning Area capacity Increase Substation Project Proponent's Environmental Assessment: Section 16 Corona and induced current effects, No report number given*," pp. 7.

Petovello, M.G., C. O'Driscoll, G. Lachapelle, D. Borio and H. Murtaza (2009) "Architecture and Benefits of an Advanced GNSS Software Receiver," *Positioning*, 1, 1, pp. 66-78.

Phillips, D. (2007) "Corona Tutorial," *Presented at IEEE Joint Technical Committee Meeting*, San Diego CA, pp. 22.